Nonlinear Dyn (2024) 112:13995–14018
https://doi.org/10.1007/s11071-024-09822-2

RESEARCH

Efficient path integral approach via analytical asymptotic expansion for nonlinear systems under Gaussian white noise

Alberto Di Matteo · Antonina Pirrotta

Received: 12 February 2024 / Accepted: 29 May 2024 / Published online: 5 June 2024

Abstract In this paper an efficient formulation of the Path integral (PI) approach is developed for determining the response probability density functions (PDFs) and first-passage statistics of nonlinear oscillators subject to stationary and time-modulated external Gaussian white noise excitations. Specifically, the evolution of the response PDF is obtained in short time steps, by using a discrete version of the Chapman-Kolmogorov equation and assuming a Gaussian form for the conditional response PDF. Next, the technique involves proceeding to treating the problem via an analytical asymptotic expansion procedure, namely the Laplace's method of integration. In this manner, the repetitive double integrals involved in the standard implementation of the PI approach are evaluated in a closed form, while the response and first-passage PDFs are obtained by mundane step-by-step application of the derived approximate analytical expression. It is shown that the herein proposed formulation can drastically decrease the associated computational cost by several orders of magnitude, as compared to both the standard PI technique and Monte Carlo solution (MCS) approach. A number of nonlinear oscillators are considered in the numerical examples. Notably, for these systems both response PDFs and first-passage probabilities are presented, whereas comparisons with pertinent MCS data demonstrate the efficiency and accuracy of the technique.

Keywords Path integral approach · Laplace's method of integration · Stochastic response · Survival probability · Nonlinear systems

A. Di Matteo (✉) · A. Pirrotta
Department of Engineering, University of Palermo, viale delle Scienze, 90128 Palermo, Italy
e-mail: alberto.dimatteo@unipa.it

A. Pirrotta
e-mail: antonina.pirrotta@unipa.it

1 Introduction

Structural and mechanical systems in many engineering fields are often subject to excitations such as winds, seismic motions, and ocean waves, whose realistic modeling necessitates their representation by nonstationary stochastic processes. Further, in many cases, these systems may include complex nonlinearites that arise due to various factors, such as material hysteresis, friction in structural joints and solid–fluid interaction forces. In this context, the problem of the response determination of systems comprising nonlinear/hysteretic terms under random excitations represents, indeed, a persistent challenge in the area of modern stochastic engineering mechanics. Clearly, Monte Carlo simulations (MCS) based approaches are among the most versatile tools for determining the response statistics of arbitrary stochastic systems (e.g. [1,2]). In many instances, however, especially for large-scale complex systems, MCS techniques can be computationally costly. In this regard, various alternative approaches have been adopted in

the literature, for instance resorting to the tools of statistical linearization [2–4] and stochastic averaging [5,6], Wiener Path Integral approaches [7,8], Galerkin scheme-based procedures [9], and moment equation procedures [10,11]. Further, recent attempts to address this problem by deriving approximate analytical representations of the stationary response probability density functions (PDFs) can be found in [12,13].

A related problem of considerable interest for safety and risk assessment pertains to the determination of the so-called survival probability of the system. That is, the probability the system response stays within a prescribed domain within a specified time interval. An alternative equivalent definition, namely the first-passage problem, represents its counterpart. This refers to the evaluation of the probability that the response of the system reaches, and possibly crosses, a predetermined level for the first time. In this regard, derivations of exact solutions are reported in [14], while examples of numerical or semi-analytical procedures to address this problem can be found in [15–18].

In this context, the so-called Path Integral (PI) approach represents an alternative method that yields accurate estimates of the response PDF and reliability statistics typically of low-dimensional nonlinear systems. In essence, the PI approach constitutes a discrete version of the well-known Chapman-Kolmogorov (CK) equation, which is associated with Markov processes [19,20]. The main concept of the approach is that the evolution of the response PDF is computed in short time steps, assuming a Gaussian form for the conditional response PDF. Specifically, the response PDF at a certain time instant can be computed simply by evaluating an integral whose kernel involves the response PDF in a previous time instant, and the conditional PDF (CPDF) of the system. Since the seminal contributions in [21–23], where the method's numerical implementation was first addressed, the PI approach has been widely employed across various engineering domains [24]. Typically the PI approach has been used for the evaluation of the stochastic response of systems subject to stationary and time-modulated normal white noise excitation [25–30]. Further advancements have extended the method to address reliability analyses [18,25,31,32], even considering the case of non-normal excitations, such as Poisson, Lèvy white noises and parametric excitations [33–40]. Notably, for low-dimensional systems the PI approach can be significantly more efficient than MCS. However, its standard implementation proves computationally costly for relatively high-dimensional MDOF systems. In this regard, several different numerical schemes have been proposed in the literature to expedite the computation of the integrals involved in the CK equation, such as Gauss-Legendre scheme [41] which can be coupled with non-Gaussian form of the transition PDF [42], Fourier series based approach [43], Fast Gauss Transform implemented within the short-time Gaussian approximation of the CPDF [44], spline interpolation of the log-PDF [29], and Generalized Cell Mapping method [45]. Further, recent research efforts have focused on developing efficient implementation strategies for the PI approach tailored to MDOF systems, for instance based on GPU computing and parallelization procedures [46–52]. Readers may also refer to [53] for a comprehensive review on the PI method.

Although significant progresses have been achieved in this domain, the high computational effort required by the PI approach still represents a sustained challenge. Nevertheless, the advantageous features of the technique, such as its accuracy even at low probability levels and its applicability to virtually any type of nonlinearity, warrant additional exploration into alternative implementations of the PI approach.

In this context, a potential approach could involve employing an approximate analytical asymptotic expansion treatment of the integrals within the CK equations. This technique, commonly referred to as Laplace's method of integration, is a mathematical tool frequently utilized to derive approximate closed-form solutions for integrals containing exponential functions in their kernels [54,55]. Recently, the aforementioned technique has been used in combination with the PI approach for determining the stochastic response of nonlinear single-degree-of-freedom (SDOF) systems [56] also endowed with fractional derivatives elements [57]. However, in all these cases this has been achieved by approximately modeling the oscillator response amplitude as a one-dimensional Markovian process, using a combination of statistical linearization and stochastic averaging methods.

In this regard, in this paper, the PI approach formulation/implementation based on the Laplace's method of integration is generalized and extended to cope with nonlinear SDOF systems subject to stationary and time-modulated white noise excitation. Notably, this enhanced version of the PI approach circumvents approximations associated with the stochastic averag-

ing/linearization treatment previously employed. Specifically, the Laplace's method directly yields an approximate closed-form solution of the double integrals involved in the standard implementation of the PI approach.

In this regard, it is noted that the proposed approach substantially differs from other techniques aimed at improving the performance of the PI method. Specifically, while these approaches, as previously mentioned, relied on different schemes for numerically computing the integrals involved in the CK equation, here the Laplace's method of integration is exploited to directly yield an approximate analytical solution of these integrals. In this manner, the repetitive integration, required by the classical numerical implementation of the PI approach for each time step, can be circumvented and the evolution of the response PDF is performed by a direct application of the obtained approximate analytical expression.

Further, for the first time the Laplace's method-based PI approach is extended to perform reliability analyses. In this manner, the evolution of the response PDFs and first-passage probabilities of a broad class of nonlinear oscillators are determined. It is shown that the herein proposed implementation can drastically decrease the associated computational cost by several orders of magnitude. Several numerical examples are included to illustrate the versatility of the approach, comprising the Duffing and the self-excited (Van der Pol-Rayleigh) oscillators, a nonlinear ship rolling motion system, and a strongly nonlinear system with signum-type nonlinearity. Finally, comparisons with pertinent MCS data demonstrate the efficiency and accuracy of the approach.

2 Mathematical background on the Path Integral approach

Consider an SDOF nonlinear system whose equation of motion can be written as

$$\ddot{X}(t) + f(X, \dot{X}, t) = V(t) \tag{1}$$

where a dot over a variable denotes differentiation with respect to time t, and $f(X, \dot{X}, t)$ is an arbitrarily chosen nonlinear deterministic function of $X(t)$ and $\dot{X}(t)$. Further, $V(t)$ is a modulated white noise process, $V(t) = \chi(t)W(t)$, where $\chi(t)$ is a deterministic modulating function and $W(t)$ is a zero-mean stationary Gaussian white noise with constant (two-sided) power spectral density S_0. Thus, the time-dependent spectral density of the process $V(t)$ is given as

$$S_V(t) = \chi^2(t) S_0. \tag{2}$$

Note that here modulated white noise excitation is considered to model the case of nonstationary stochastic excitations. Clearly, the more simple case of stationary Gaussian white noise is retrieved by assuming $\chi(t) = 1$.

Further, it is assumed that the initial conditions of the system in Eq. (1), $X(0) = X_0$ and $\dot{X}(0) = \dot{X}_0$, can be either deterministic or random variables with assigned PDF $p_{X_0\dot{X}_0}$.

The system in Eq. (1) can be rewritten in terms of state variables as

$$\dot{\mathbf{Z}}(t) = \mathbf{f}(\mathbf{Z}, t) + \mathbf{l}V(t) \tag{3}$$

where $\mathbf{Z}(t) = [Z_1(t)\ Z_2(t)]^T = [X(t)\ \dot{X}(t)]^T$, $\mathbf{l} = [0\ 1]^T$, and

$$\mathbf{f}(\mathbf{Z}, t) = \begin{bmatrix} Z_2 \\ -f(Z_1, Z_2, t) \end{bmatrix}. \tag{4}$$

Based on Eq. (3), $\mathbf{Z}(t)$ is a two-dimensional Markov vector process that satisfies the CK equation

$$p_{\mathbf{Z}}(\mathbf{z}, t+\tau) = \int_{-\infty}^{\infty}\int_{-\infty}^{\infty} p_{\mathbf{Z}}(z_1, z_2, t+\tau|\bar{z}_1, \bar{z}_2, t)\, p_{\mathbf{Z}}(\bar{z}_1, \bar{z}_2, t)\, d\bar{z}_1\, d\bar{z}_2, \tag{5}$$

where for compactness $p_{\mathbf{Z}}(\mathbf{z}, t+\tau) = p_{\mathbf{Z}}(z_1, z_2, t+\tau)$, and $p_{\mathbf{Z}}(z_1, z_2, t+\tau|\bar{z}_1, \bar{z}_2, t)$ is the so-called Conditional PDF (CPDF) of the response vector process $\mathbf{Z}(t)$.

Equation (5) represents the basis of the PI approach. Specifically, as it can be seen, the PDF of the response process $p_{\mathbf{Z}}(z_1, z_2, t+\tau)$ at the time instant $(t+\tau)$ can be evaluated by solving a double-integral whose kernel involves the CPDF for assigned (deterministic) initial condition $(\bar{z}_1, \bar{z}_2)$ in t, and the PDF of the response process in a previous time instant t.

Note that, although Eq. (5) holds for any value of τ, if τ is sufficiently small, the sought CPDF approximately follows a Gaussian distribution [27]. Further, as shown in [27], the CPDF $p_{\mathbf{Z}}(z_1, z_2, t+\tau|\bar{z}_1, \bar{z}_2, t)$ in Eq. (5) can be obtained by evaluating the unconditional PDF in τ of the process $\bar{\mathbf{Z}}(\rho)$ governed by the differential equation

$$\dot{\bar{\mathbf{Z}}}(\rho) = \mathbf{f}(\bar{\mathbf{Z}}, \rho) + \mathbf{l}V(t+\rho);\ 0 \le \rho \le \tau \tag{6}$$

associated with the initial conditions $\bar{\mathbf{Z}}(0) = [\bar{z}_1\ \bar{z}_2]^T$. That is,

$$p_{\mathbf{Z}}(z_1, z_2, t+\tau|\bar{z}_1, \bar{z}_2, t) = p_{\bar{\mathbf{Z}}}(\bar{\mathbf{z}}, \tau) \tag{7}$$

In this regard, Eq. (6) can be rewritten as

$$\begin{cases} \dot{\bar{Z}}_1(\rho) = \bar{Z}_2(\rho) \\ \dot{\bar{Z}}_2(\rho) = -f(\bar{Z}_1, \bar{Z}_2) + V(t+\rho)\ \cdot \\ \bar{Z}_1(0) = \bar{z}_1;\ \bar{Z}_2(0) = \bar{z}_2 \end{cases} \tag{8}$$

Evaluating Eq. (8) in τ, and assuming τ sufficiently small, yields

$$\bar{Z}_1(\tau) = \bar{z}_1 + \bar{z}_2\tau = \mu_1(\bar{z}_1, \bar{z}_2), \tag{9}$$

which is a deterministic function. Thus, the distribution in τ of the process $\bar{Z}_1(\rho)$ is a Dirac's delta centered in $\mu_1(\bar{z}_1, \bar{z}_2)$. That is,

$$p_{\bar{z}_1}(z_1, \tau) = \delta[z_1 - (\bar{z}_1 + \bar{z}_2\tau)]. \tag{10}$$

As far as the process $\bar{Z}_2(\rho)$ is concerned, as shown in [27,44], Eq. (8) for small τ yields

$$\bar{Z}_2(\tau) = \bar{z}_2 - f(\bar{z}_1, \bar{z}_2)\tau + G\tau^{1/2}, \tag{11}$$

where G is a zero-mean normal random variable with variance $E[G^2] = q(t) = 2\pi S_V(t)$, and $E[\cdot]$ is the mathematical expectation operator. Therefore, the mean value and the variance of $\bar{Z}_2(\tau)$ can be given respectively as

$$E[\bar{Z}_2(\tau)] = \bar{z}_2 - f(\bar{z}_1, \bar{z}_2)\tau = \mu_2(\bar{z}_1, \bar{z}_2), \tag{12}$$

and

$$\sigma^2_{\bar{Z}_2}(\tau) = E[\bar{Z}_2^2(\tau)] - E[\bar{Z}_2(\tau)]^2 = q(t)\tau. \tag{13}$$

Note that the variable $\bar{z}_1$ is deterministic, and the two processes $\bar{Z}_1$ and $\bar{Z}_2$ are independent. In this manner, as shown in [27,30], taking into account Eq. (7), the complete CPDF in Eq. (5) can be given as

$$p_{\mathbf{Z}}(z_1, z_2, t+\tau|\bar{z}_1, \bar{z}_2, t) = \frac{\delta[z_1 - (\bar{z}_1 + \bar{z}_2\tau)]}{\sqrt{2\pi q(t)\tau}} \exp\left(-\frac{(z_2 - \mu_2(\bar{z}_1, \bar{z}_2))^2}{2q(t)\tau}\right). \tag{14}$$

Further, by inserting Eq. (14) into Eq. (5) and taking into account the sampling property of the Dirac's delta function, Eq. (5) can be rewritten as

$$p_{\mathbf{Z}}(\mathbf{z}, t+\tau) = \frac{1}{\sqrt{2\pi q(t)\tau}} \int_{-\infty}^{\infty} \exp\left(-\frac{(z_2 - \mu_2(z_1 - \bar{z}_2\tau, \bar{z}_2))^2}{2q(t)\tau}\right) p_{\mathbf{Z}}(z_1 - \bar{z}_2\tau, \bar{z}_2, t)\, d\bar{z}_2. \tag{15}$$

Equation (15) represents the final form of the PI approach for nonlinear systems excited by modulated Gaussian white noise processes. Note that, with respect to Eqs. (5), (15) requires only the solution of a single integral. Generally a discretized version of Eq. (15) is implemented. In this regard, consider the time interval $[0, t_f]$, where t_f is the final time instant, discretized so that the generic time instant is $t_k = k\Delta t$ where $(k = 0, ..., N)$ and $\Delta t = t_f/N$ is a small time step. Then, Eq. (15) can be rewritten as

$$p_{\mathbf{Z},k+1}(\mathbf{z}) = \frac{1}{\sqrt{2\pi q_k \Delta t}} \int_{-\infty}^{\infty} \exp\left[-\frac{(z_2 - \mu_2(z_1 - \bar{z}_2\Delta t, \bar{z}_2))^2}{2q_k\Delta t}\right] p_{\mathbf{Z},k}(z_1 - \bar{z}_2\Delta t, \bar{z}_2)\, d\bar{z}_2. \tag{16}$$

where for compactness $p_{\mathbf{Z},k+1}(\mathbf{z}) = p_{\mathbf{Z}}(z_1, z_2, t_{k+1})$, and $q_k = q(t_k)$.

It can be readily seen from this equation that a step-by-step application of Eq. (16) yields the entire evolution of the response PDF $p_{\mathbf{Z},k}(\mathbf{z})$. However, this requires a repetitive numerical integration in the $\bar{z}_2$ domain for each time step, which often constitutes the highest contribution to the computational cost of the method itself, especially for higher dimensional systems. Further, it is pointed out that the integral in Eq. (16) involves the determination of the response PDF in the previous time instant t_k evaluated at the points $(z_1 - \bar{z}_2\Delta t, \bar{z}_2)$, which do not coincide with the points in the domain (z_1, z_2) of the known PDF $p_{\mathbf{Z},k}(\mathbf{z})$. On this basis, for each time step an interpolation procedure is necessary, for instance using cubic B-splines, to compute the required values of the PDF.

3 Path Integral approach via Laplace's method of integration

Examining the particular form of the integral in Eq. (16), it can be argued that an approximate closed-form solution of this integral could be derived by an asymptotic expansion treatment employing the Laplace's method of integration, as detailed in the Appendix A.

In this regard, note that a small time-step Δt is commonly adopted in the standard implementation of the PI approach (often smaller than 10^{-2}) s, and generally

the functions in the kernel of the integral in Eq. (16) are sufficiently smooth. Thus, following Appendix A, an approximate solution of Eq. (16) can be derived based on Eq. (A5). Specifically, Eq. (16) can be rewritten as

$$p_{\mathbf{Z},k+1}(\mathbf{z}) = \frac{1}{\sqrt{2\pi q_k \Delta t}} \int_{-\infty}^{\infty} p_{\mathbf{Z},k}(z_1 - \bar{z}_2 \Delta t, \bar{z}_2) \exp\left[-\frac{\lambda}{q_k} g(\mathbf{z}, \bar{z}_2)\right] d\bar{z}_2, \tag{17}$$

where

$$g(\mathbf{z}, \bar{z}_2) = g(z_1, z_2, \bar{z}_2) = [z_2 - \mu_2(z_1 - \bar{z}_2 \Delta t, \bar{z}_2)]^2, \tag{18}$$

and $\lambda = 1/(2\Delta t)$, with $\lambda \gg 0$.

In this manner Eq. (17) is given in a form similar to Eq. (A1) and the Laplace's method of integration can be applied. In this regard, denote as $\bar{z}_2^*$ the value of $\bar{z}_2$ such that

$$\left.\frac{\partial g(\mathbf{z}, \bar{z}_2)}{\partial \bar{z}_2}\right|_{\bar{z}_2 = \bar{z}_2^*} = g^I(\mathbf{z}, \bar{z}_2^*) = 0 \tag{19}$$

and

$$\left.\frac{\partial^2 g(\mathbf{z}, \bar{z}_2)}{\partial^2 \bar{z}_2}\right|_{\bar{z}_2 = \bar{z}_2^*} = g^{II}(\mathbf{z}, \bar{z}_2^*) > 0 \tag{20}$$

where the apexes (I) and (II) stand for the order of the derivatives with respect to $\bar{z}_2$.

Then, taking into account Eqs. (A5), the approximate analytical solution of the CK equation Eq. (16) can be given as

$$p_{\mathbf{Z},k+1}(\mathbf{z}) = \sqrt{\frac{2}{g^{II}(\mathbf{z}, \bar{z}_2^*)}} e^{-\frac{\lambda}{q_k} g(\mathbf{z}, \bar{z}_2^*)} \left[\bar{p}_{\mathbf{Z},k}(z_1, \bar{z}_2^*) + \frac{q_k}{2\lambda g^{II}(\mathbf{z}, \bar{z}_2^*)} \bar{p}^{II}_{\mathbf{Z},k}(z_1, \bar{z}_2^*)\right] \tag{21}$$

where, for compactness,

$$\bar{p}_{\mathbf{Z},k}(z_1, \bar{z}_2^*) = p_{\mathbf{Z}}(z_1 - \bar{z}_2^* \Delta t, \bar{z}_2^*, t_k) \tag{22}$$

and

$$\bar{p}^{II}_{\mathbf{Z},k}(z_1, \bar{z}_2^*) = \left.\frac{\partial^2 p_{\mathbf{Z},k}(z_1 - \bar{z}_2 \Delta t, \bar{z}_2)}{\partial \bar{z}_2^2}\right|_{\bar{z}_2 = \bar{z}_2^*} \tag{23}$$

Notably, the significance of Eq. (21) relates to the fact that the evolution of the response PDF of the nonlinear system in Eq. (1) can be readily computed via a step-by-step application of this approximate analytical expression. Clearly, in this manner, the computationally demanding repetitive numerical integrations involved in Eq. (15) are avoided.

Further, it is worth mentioning that Eq. (21) is based on a second-order expansion of the kernel in Eq. (16), and this generally yields a reasonable level of accuracy. Nevertheless, if necessary higher accuracy can be achieved by employing a fourth-order expansion as in Eq. (A6), leading to

$$\begin{aligned} p_{\mathbf{Z},k+1}(\mathbf{z}) = & \sqrt{\frac{2}{g^{II}(\mathbf{z}, \bar{z}_2^*)}} e^{-\frac{\lambda}{q_k} g(\mathbf{z}, \bar{z}_2^*)} \cdot \left\{ \bar{p}_{\mathbf{Z},k}(z_1, \bar{z}_2^*) + \frac{q_k}{\lambda} \left[\frac{\bar{p}^{II}_{\mathbf{Z},k}(z_1, \bar{z}_2^*)}{2 g^{II}(\mathbf{z}, \bar{z}_2^*)} \right.\right. \\ & - \frac{\bar{p}_{\mathbf{Z},k}(z_1, \bar{z}_2^*)}{8} \frac{g^{IV}(\mathbf{z}, \bar{z}_2^*)}{g^{II}(\mathbf{z}, \bar{z}_2^*)^2} \cdot \\ & - \frac{\bar{p}^{I}_{\mathbf{Z},k}(z_1, \bar{z}_2^*)}{2} \frac{g^{III}(\mathbf{z}, \bar{z}_2^*)}{g^{II}(\mathbf{z}, \bar{z}_2^*)^2} \\ & \left.\left. + \frac{5 \bar{p}_{\mathbf{Z},k}(z_1, \bar{z}_2^*)}{24} \frac{g^{III}(\mathbf{z}, \bar{z}_2^*)^2}{g^{II}(\mathbf{z}, \bar{z}_2^*)^3} \right] \right\} \end{aligned} \tag{24}$$

Finally, as far as the implementation of Eqs. (21) or (24) is concerned, note that the function $\bar{p}_{\mathbf{Z},k}(z_1, \bar{z}_2^*)$ and its derivatives must be evaluated at each time step, for instance using an interpolation procedure based on the known response PDF $p_{\mathbf{Z},k}(z_1, z_2)$ and taking into account Eq. (22). On the other hand, $g(\mathbf{z}, \bar{z}_2^*)$, in Eq. (18), and its derivatives are deterministic functions, independent of the PDF of the response process. Therefore, they can be computed separately once beforehand, together with the values $\bar{z}_2^*$ satisfying Eqs. (19) and (20), hence further reducing the computational effort.

4 First-passage probability

The first-passage problem refers to the determination of the probability that the various trajectories of the stochastic process $\mathbf{Z}(t)$, solution of Eq. (1), cross a prescribed safe domain for the first time, within a certain time interval $[0, T]$. Note that, as shown in [37], the first-passage problem can be efficiently and accurately addressed based on a modification of the PI approach.

In this regard, without loss of generality, assume that only the barrier crossing of the displacement process $Z_1(t) = X(t)$ is of interest and denote as $[\eta, \xi]$ the threshold barriers of the prescribed safe domain. Next, discretize the time interval $[0, T]$ into sufficiently small steps Δt. In this manner, it can be assumed that Eq. (14) holds true, and all the trajectories of the process

$Z_1(t)$ with deterministic initial condition ($z_1 = \bar{z}_1$) are monotone in the generic interval $[t_k\,, t_k + \Delta t]$.

Further, consider the classical absorbing barrier problem. That is, it is assumed that each trajectory is canceled upon reaching the prescribed threshold. On this basis, a new function denoted as Reliability Density Function (RDF) $r_{\xi\eta}(z_1, z_2, t_{k+1})$ may be introduced as [37]

$$r_{\xi\eta,k+1}(\mathbf{z}) = U(z_1-\eta)U(\xi-z_1) \int_{-\infty}^{\infty}\int_{\eta}^{\xi} p_{\mathbf{Z}}(\mathbf{z}, t_{k+1}|\bar{\mathbf{z}}, t_k)\; r_{\xi\eta,k}(\bar{\mathbf{z}})\, d\bar{z}_1\, d\bar{z}_2, \tag{25}$$

where $p_{\mathbf{Z}}(\mathbf{z}, t_{k+1}|\bar{\mathbf{z}}, t_k)$ is the CPDF, defined in Eq. (14) for small time intervals $\tau = \Delta t$, $U(\cdot)$ is the unit step function, and $q_{\xi\eta,0}(\mathbf{z}) = U(z_1-\eta)U(\xi-z_1)p_{X_0\dot{X}_0}$.

Note that the function $r_{\xi\eta,k}(\mathbf{z})$ cannot be considered a PDF since its area is not unitary. Nevertheless, it represents the probability that the trajectories of the response process $\mathbf{Z}(t)$ fall, at the generic time instant $(t_k + \Delta t)$ in the interval $[\mathbf{z}, \mathbf{z} + d\mathbf{z}]$.

Clearly, Eq. (14) can be regarded as the modification of the PI approach for the first-passage problem. Further, once the RDF $r_{\xi\eta,k}(\mathbf{z})$ is evaluated, the so-called reliability function $R_E(T)$ can be obtained. Specifically, this is defined as the probability that the system response $Z_1(t)$ stays within the threshold barrier $[\eta, \xi]$ over the time interval $[0, T]$; that is

$$R_E(T) = \int_{-\infty}^{\infty}\int_{\eta}^{\xi} r_{\xi\eta}(\mathbf{z}, T)\, dz_1\, dz_2, \tag{26}$$

In this manner, the so-called first-passage probability $P_E(T)$, namely the probability that the system response crosses the barrier in the time interval $[0, T]$, can be simply obtained as the complementary to one of $R_E(T)$. Finally, the corresponding first-passage time PDF, that is the time at which the response process $Z_1(t)$ crosses the barrier for the first time, is obtianed as

$$p_E(T) = -\frac{dR_E(T)}{dT} \tag{27}$$

4.1 First-passage problem by Laplace's method

Notably, following the procedure previously discussed for the response PDF, an approximate analytical solution of Eq. (25) could be obtained by resorting to an asymptotic expansion treatment of the integrals based on the Laplace's method of integration. In this regard, substituting Eq. (14) into Eq. (25) yields

$$r_{\xi\eta,k+1}(\mathbf{z}) = \frac{U(z_1-\eta)U(\xi-z_1)}{\sqrt{2\pi q_k \Delta t}} \int_{-\infty}^{\infty}\int_{\eta}^{\xi} \exp\left(-\frac{(z_2-\mu_2(\bar{\mathbf{z}}))^2}{2q_k\Delta t}\right) \delta[z_1-(\bar{z}_1+\bar{z}_2\Delta t)]\; r_{\xi\eta,k}(\bar{\mathbf{z}})\, d\bar{z}_1\, d\bar{z}_2, \tag{28}$$

Next, taking into account the sampling property of the Dirac's delta function, after mundane manipulations, Eq. (28) yields

$$r_{\xi\eta,k+1}(\mathbf{z}) = \frac{U(z_1-\eta)U(\xi-z_1)}{\sqrt{2\pi q_k \Delta t^3}} \int_{\eta}^{\xi} \exp\left[-\frac{\lambda}{q_k}h(\mathbf{z}, \bar{z}_1)\right] r_{\xi\eta,k}\left(\bar{z}_1, \frac{z_1-\bar{z}_1}{\Delta t}\right) d\bar{z}_1, \tag{29}$$

where

$$h(\mathbf{z}, \bar{z}_1) = \left[z_2 - \mu_2\left(\bar{z}_1, \frac{z_1-\bar{z}_1}{\Delta t}\right)\right]^2 \tag{30}$$

in which $\mu_2(z_1, z_2)$ is given in Eq. (12).

As it can be seen, Eq. (29) only involves a single integral in the $\bar{z}_1$ domain. This can be evaluated again by utilizing the Laplace's method of integration. Specifically, considering the variable change $\bar{z}_2 = (z_1 - \bar{z}_1)/\Delta t$, Eq. (29) is simply rewritten as

$$r_{\xi\eta,k+1}(\mathbf{z}) = \frac{U(z_1-\eta)U(\xi-z_1)}{\sqrt{2\pi q_k \Delta t}} \int_{\eta}^{\xi} \exp\left[-\frac{\lambda}{q_k}g(\mathbf{z}, \bar{z}_2)\right] r_{\xi\eta,k}\,(z_1-\bar{z}_2\Delta t, \bar{z}_2)\; d\bar{z}_2, \tag{31}$$

where $g(\mathbf{z}, \bar{z}_2)$ is given in Eq. (18). In this manner, an expression analogous to Eq. (17) is obtained. Thus, denote as $\bar{z}_2^*$ the value of $\bar{z}_2$, in the interval $[\eta, \xi]$, satisfying the conditions in Eqs. (19) and (20). Taking into account Eq. (A5), the approximate analytical solution of the integral in Eq. (31) can be given as

$$r_{\xi\eta,k+1}(\mathbf{z}) = U(z_1-\eta)U(\xi-z_1)\frac{\sqrt{2}\,e^{-\frac{\lambda}{q_k}g(\mathbf{z},\bar{z}_2^*)}}{\sqrt{g^{II}(\mathbf{z}, \bar{z}_2^*)}} \left[\bar{r}_{\xi\eta,k}(z_1, \bar{z}_2^*) + \frac{q_k}{2\lambda\, g^{II}(\mathbf{z}, \bar{z}_2^*)}\bar{r}^{II}_{\xi\eta,k}(z_1, \bar{z}_2^*)\right] \tag{32}$$

where, similarly to Eqs. (22) and (23),

$$\bar{r}_{\xi\eta,k}(z_1,\bar{z}_2^*) = r_{\xi\eta}\big(z_1-\bar{z}_2^*\Delta t,\bar{z}_2^*,t_k\big) \tag{33}$$

and

$$\bar{r}^{II}_{\xi\eta,k}(z_1,\bar{z}_2^*) = \frac{\partial^2}{\partial\bar{z}_2^2} r_{\xi\eta}\big(z_1-\bar{z}_2^*\Delta t,\bar{z}_2^*,t_k\big)\bigg|_{\bar{z}_2=\bar{z}_2^*}. \tag{34}$$

Note that, as for Eq. (21), the significance of Eq. (32) relates to the fact that the RDF $r_{\xi\eta,k+1}(\mathbf{z})$ of the nonlinear system in Eq. (1) can be readily computed via a repetitive application of this approximate analytical expression. Thus, the computationally demanding double numerical integrations in Eq. (28) are avoided.

Finally, as far as the implementation of Eq. (32) is concerned, note that the function $g(\mathbf{z},\bar{z}_2^*)$ in Eq. (32) and the values $\bar{z}_2^*$ are deterministic and have been previously employed for the determination of the response PDF in Eq. (21). Thus, they have been computed in closed-form, once beforehand, further reducing the computational cost of the procedure.

5 Numerical applications

In this section, the versatility and efficiency of the developed technique are demonstrated by various numerical examples. Specifically, three different nonlinear systems with a bimodal response PDF are considered, as well as a strongly nonlinear system possessing a signum type nonlinearity [28].

In these examples the initial PDF has been assumed as $p_{X_0\dot{X}_0} = p_{X_0}p_{\dot{X}_0}$ where p_{X_0} and $p_{\dot{X}_0}$ are Gaussian distributions with standard deviation equals to 0.2.

For each case, both the evolution of the system response PDF and the first-passage probability are determined. Analyses are carried out taking into account both stationary and nonstationary excitations, employing a time-modulating function of the exponential type, as

$$\chi(t) = 4\left[\exp\left(\frac{t}{4}\right)-\exp\left(\frac{t}{2}\right)\right]. \tag{35}$$

As far as the numerical implementation of the proposed approach is concerned, Eq. (21) has been used since it generally leads to a sufficient degree of accuracy, employing a time step ($\Delta t = 5\cdot 10^{-3}$ s). Further, for each case the domain of the PDF has been uniformly divided using intervals of ($\Delta x = \Delta\dot{x} = 5\cdot 10^{-2}$) and standard interpolation based on cubic polynomials has been employed for determining $\bar{p}_{\mathbf{Z},k}(z_1,\bar{z}_2^*)$ in Eq. (21) at each time step.. In addition, pertinent MCS data have been obtained considering, for each case, 50000 samples for the evolution of the response PDF, and 10^6 samples for an accurate determination of the first-passage probabilities.

5.1 Duffing oscillator

Consider first an SDOF Duffing nonlinear oscillator, whose equation of motion is given in Eq. (21) where the nonlinear function $f(X,\dot{X},t)$ takes the form

$$f(X,\dot{X},t) = \beta\dot{X} + k_0X + \epsilon X^3. \tag{36}$$

where β and k_0 are the damping and stiffness coefficients, respectively, while ϵ is a constant describing the magnitude of the nonlinearity.

Note that the stationary joint response PDF of the Duffing oscillator subject to a stationary Gaussian white noise with constant PSD S_0 has an analytical expression (e.g., [58]) of the form

$$p_{X\dot{X}}(x,\dot{x}) = C\exp\left[-\frac{\beta}{\pi S_0}\left(\frac{k_0x^3}{2}+\frac{\epsilon x^4}{4}+\frac{\dot{x}}{2}\right)\right], \tag{37}$$

where C is a normalization constant. Following the proposed approach, taking into account Eqs. (12), (18) yields

$$\begin{aligned} g(\mathbf{z},\bar{z}_2) =& \big[z_2+3z_1\bar{z}_2^2\Delta t^3\epsilon \\ &-\bar{z}_2^3\Delta t^4\epsilon + z_1\Delta t\big(z_1^2\epsilon+k_0\big) \\ &+\bar{z}_2\big(-1+\Delta t\beta \\ &-\big(3z_1^2\epsilon+k_0\big)\Delta t^2\big)\big]^2 \end{aligned} \tag{38}$$

and the points $\bar{z}_2^*$ can be found, either analytically or numerically, using Eqs. (19) and (20). In this manner, it can be proved that $g(\mathbf{z},\bar{z}_2^*)=0$.

Analyses have been carried out considering a bimodal oscillator, obtained by utilizing a negative term k_0. Specifically, the following set of parameters has been used ($k_0=-2.25$, $\beta=0.15$, $\epsilon=6.75$, $S_0=0.3/2\pi$). In this regard, Fig. 1 shows contour plots of the evolution of the proposed PI-based response joint PDF, while in Fig. 2 corresponding marginal displacement and velocity response PDF, vis-à-vis pertinent MCS results, are reported for various time instants.

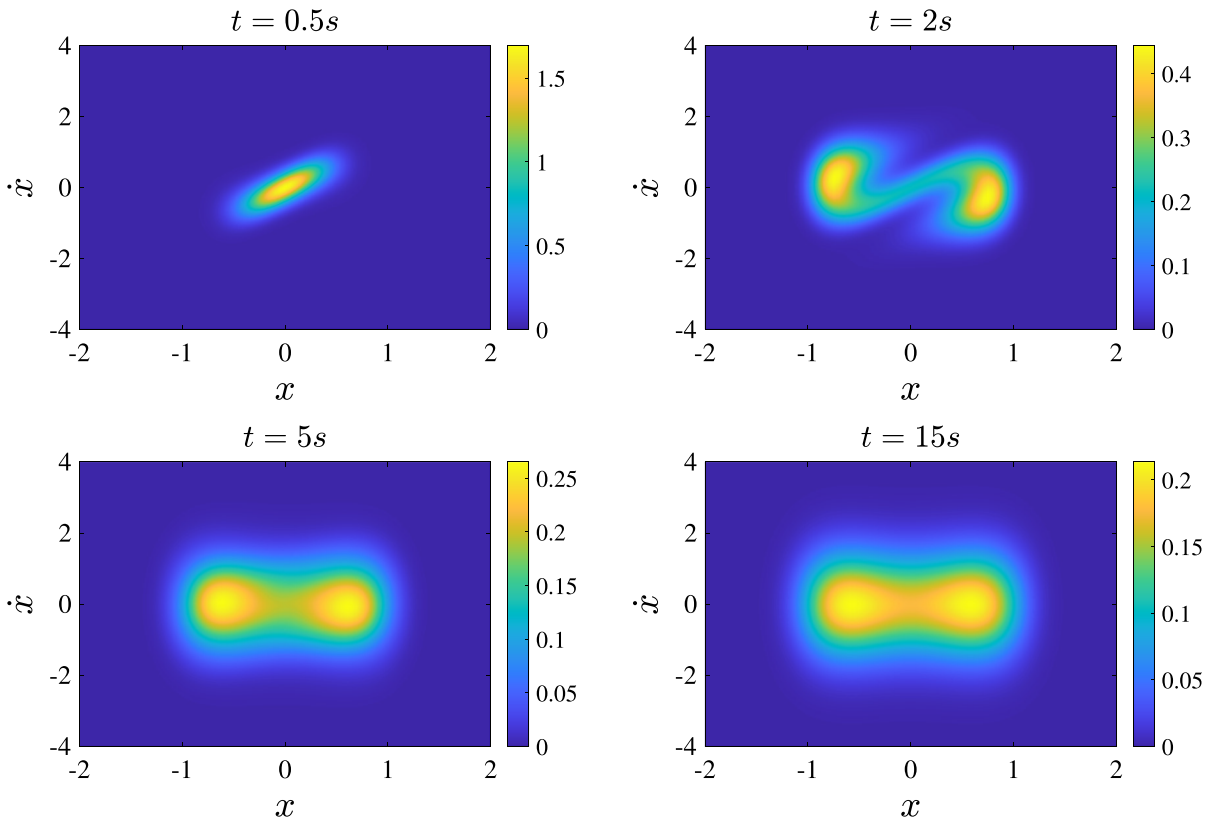

Fig. 1 Response joint PDF of the Duffing oscillator for white noise excitation. Contour plot obtained by the proposed PI approach for different time instants

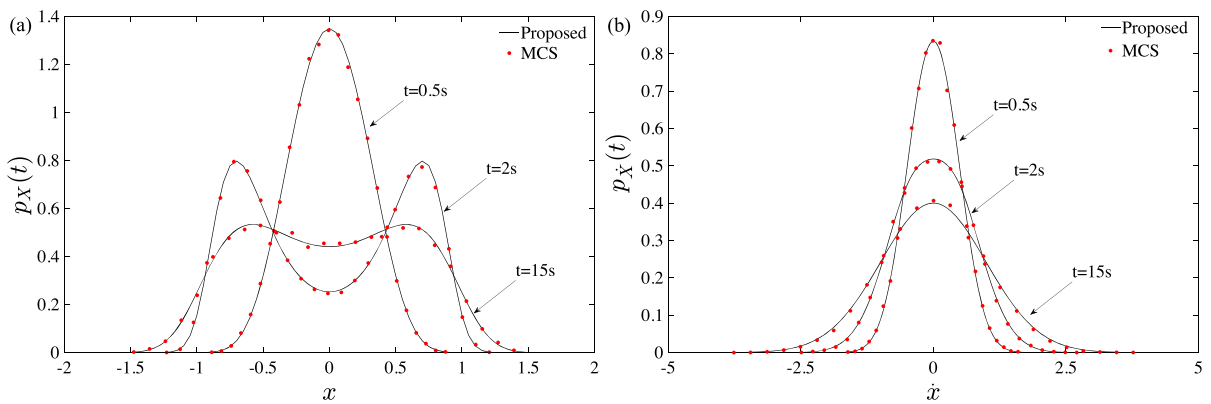

Fig. 2 Response marginal PDF of the Duffing oscillator for white noise excitation. Proposed PI approach (black lines) vis-à-vis MCS data (red dots): **a** Marginal response displacement PDF; **b** Marginal response velocity PDF

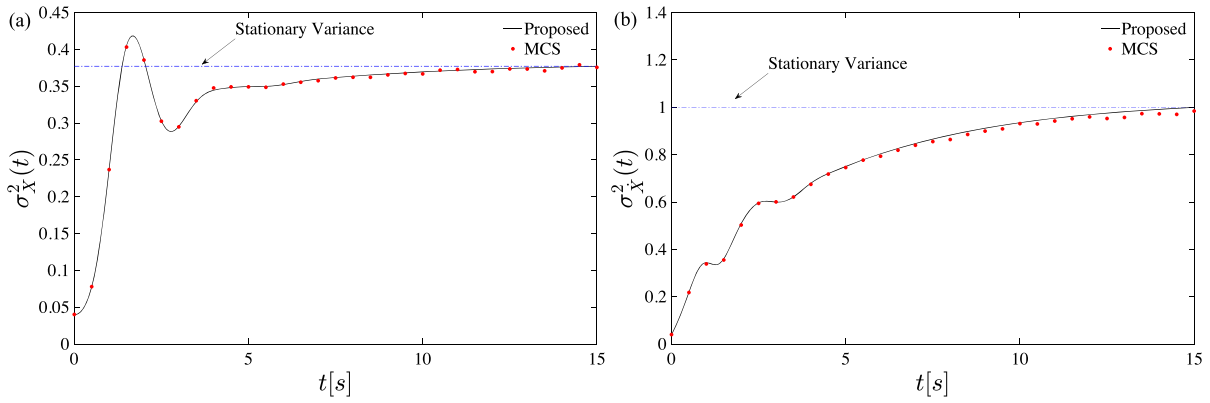

Fig. 3 Nonstationary response variances of the Duffing oscillator for white noise excitation. Proposed PI approach (black line) vis-à-vis MCS data (red dots): **a** Response displacement variance; **b** Response velocity variance

Further, in Fig. 3 the nonstationary displacement and velocity variances are plotted together with MCS estimates and stationary values obtained by using Eq. (37). As it can be seen, a very good agreement is achieved both in terms of marginal PDFs for each time instant, and response variances.

Next, analogous analyses have been carried out considering a nonstationary excitation using the modulating function in Eq. (35). In this regard, corresponding results are shown in Figs. 4 and 5. As it can be seen, comparisons with pertinent MCS demonstrate a satisfactory level of accuracy exhibited by the proposed approach.

Finally, to highlight the efficiency of the method, the computational times required by the proposed PI approach for determining the response PDF at the final time instant ($t = 15$ s), and the one related to the standard implementation of the PI technique [27], are reported in Table 1. In this regard, note that the standard PI technique has been implemented using the same discretization of the (z_1, z_2) domain, and the same value of Δt employed for the proposed PI approach. Further, the ratio between the two computational times, hereinafter referred to as efficiency ratio ε, is also shown. As detailed in Table 1, the proposed approach requires just few seconds of computations, significantly decreasing the computational cost of the standard implementation of the PI approach.

In passing, it should be mentioned that other techniques may be also followed to increase the efficiency of the standard PI approach (e.g. [46,48]). For instance, a similar problem has been addressed in [46], where the stationary response PDF of a Duffing oscillator has been determined with the execution time of the GPU parallel method and the standard PI approach given, respectively, as 30 s and 546 s.

Table 1 Computational time required by the PI procedures for calculating the response PDF of the analyzed nonlinear systems in $t = 15$ s

Nonlinear System	Proposed PI	Standard PI	ε
Duffing	7.5s	939s	125
Self-excited	4.9s	62.8s	13
Ship rolling	7.6s	1170s	154
Variable stiffness	80.7s	3595s	44

Comparison between the proposed procedure and the classical PI approach

5.2 Self-excited oscillator

Next, consider the case of a so-called self-excited oscillator with both nonlinear damping and nonlinear stiffness terms, also referred to as Van der Pol-Rayleigh oscillator [59]. In this case the nonlinear function $f(X, \dot{X}, t)$ takes the form

$$f(X, \dot{X}, t) = \eta(\dot{X}^2 + X^2 - 1)\dot{X} + X. \tag{39}$$

where η is a constant.

Note that the stationary joint response PDF of this system subject to a stationary Gaussian white noise with constant PSD S_0 has an analytical expression (e.g., [42]) of the form

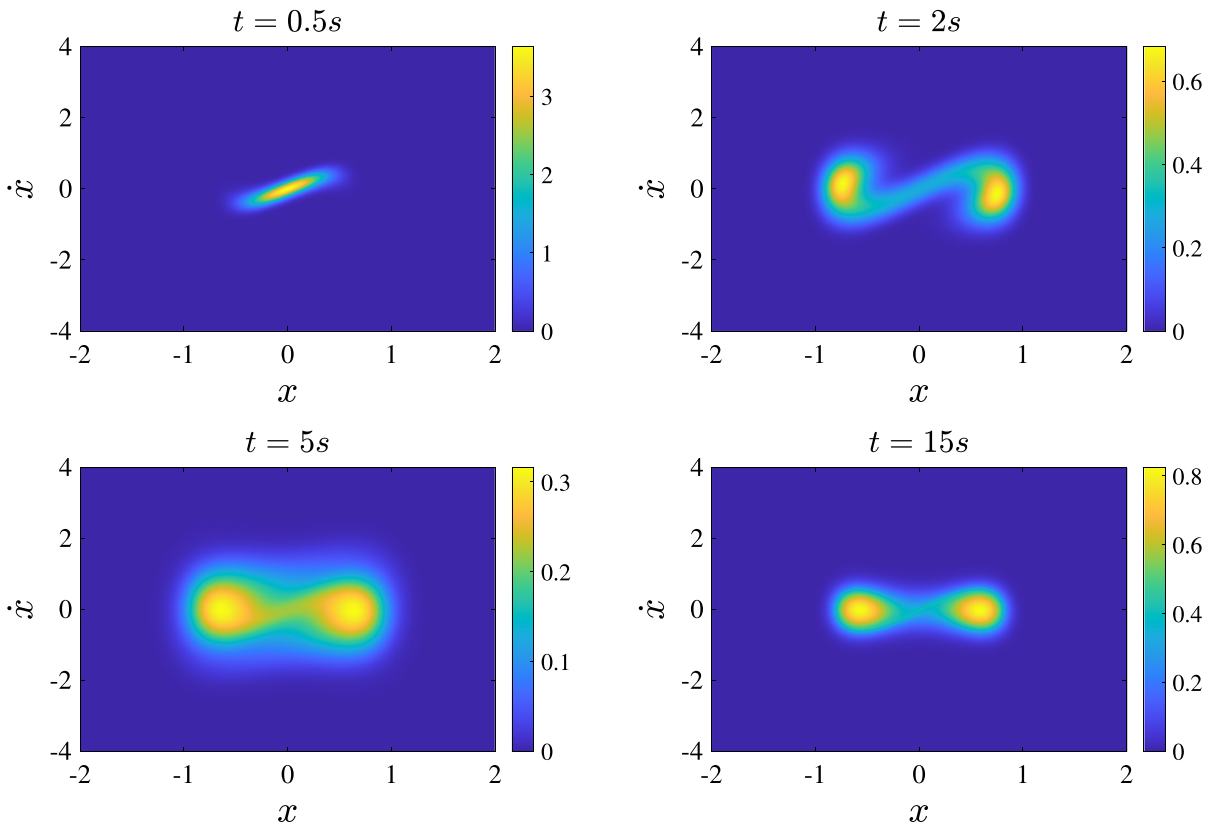

Fig. 4 Response joint PDF of the Duffing oscillator for modulated white noise excitation. Contour plot obtained by the proposed PI approach for different time instants

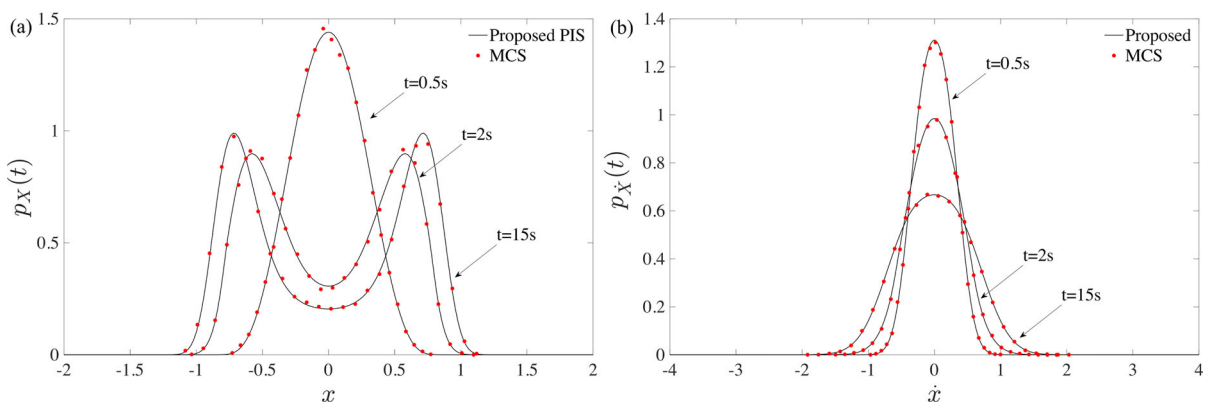

Fig. 5 Response marginal PDF of the Duffing oscillator for modulated white noise excitation. Proposed PI approach (black lines) vis-à-vis MCS data (red dots): **a** Marginal response displacement PDF; **b** Marginal response velocity PDF

$$p_{X\dot{X}}(x,\dot{x}) = C\exp\left[\frac{\eta}{\pi S_0}\left((x^2+\dot{x}^2) - \frac{(x^2+\dot{x}^2)^2}{2}\right)\right] \tag{40}$$

where C is a normalization constant.

Following the proposed approach, taking into account Eqs. (12) and (18), the function $g(\mathbf{z}, \bar{z}_2)$ is obtained as

$$\begin{aligned} g(\mathbf{z},\bar{z}_2) = 2\Big[&z_2 + z_1\Delta t - \bar{z}_2(1+\Delta t^2) \\ &+\eta\bar{z}_2\Delta t(\bar{z}_2^2 + (z_1 - \bar{z}_2\Delta t)^2 - 1)\Big] \\ &\Big[-1 - \Delta t^2 + \eta\Delta t(z_1^2 - 4z_1\bar{z}_2\Delta t \\ &+3\bar{z}_2^2(1+\Delta t^2) - 1)\Big] \end{aligned} \tag{41}$$

and the points $\bar{z}_2^*$ can be found, either analytically or numerically, using Eqs. (19) and (20).

In this regard, in Fig. 6 contour plots of the proposed PI-based response joint PDF corresponding to the parameters values in [42] ($\eta = 0.8$, $S_0 = 0.1/2\pi$) are shown for various time instants. Further, in Fig. 7 corresponding marginal displacement and velocity response PDF, vis-à-vis pertinent MCS results, are plotted. Finally, in Fig. 8 the nonstationary displacement and velocity variances are shown together with MCS estimates and stationary values obtained by using Eq. (40). It can be readily seen that the proposed PI approach yields quite accurate and reliable results, both in terms of response variances and marginal PDFs for each time instant.

As far as the efficiency of the method is concerned, note that the computational times required by the proposed approach vis-à-vis the one related to the standard implementation of the PI technique are reported in Tab. 1. As it can be seen, the proposed procedure yields a significant reduction of the computational cost, although the standard PI technique in this case is still quite efficient.

Finally, results related to the case of a nonstationary excitation, using the modulating function in Eq. (35), are shown in Figs. 9 and 10. As it can be seen, comparisons with pertinent MCS demonstrate again a satisfactory level of accuracy exhibited by the proposed approach.

5.3 Ship rolling motion

Consider the problem of the nonlinear rolling motion of a ship subject to random excitation. In this case, the nonlinear function $f(X, \dot{X}, t)$ takes the form

$$\begin{aligned} f(X,\dot{X},t) = &\beta_1\dot{X} + \beta_2|\dot{X}|\dot{X} + \alpha_1 X \\ &+\alpha_3 X^3 + \alpha_5 X^5. \end{aligned} \tag{42}$$

where α_i and β_i are defined constants.

Again, following the proposed approach, taking into account Eqs. (12) and (18), the function $g(\mathbf{z}, \bar{z}_2)$ can be obtained, and the points $\bar{z}_2^*$ are found by using Eqs. (19) and (20).

Analyses have been carried out considering the parameters in [12]; that is, ($\beta_1 = \beta_2 = 0.1, \alpha_1 = \alpha_5 = 1, \alpha_3 = -2.5, S_0 = 0.3/2\pi$).

In this regard, Fig. 11 shows contour plots of the proposed PI-based response joint PDF for different time instants, while in Fig. 12 corresponding marginal response PDF are plotted. Comparisons with pertinent MCS data reveal a satisfactory level of accuracy in each time instant for both the response marginal PDFs $p_X(t)$ and $p_{\dot{X}}(t)$.

Further, as far as the efficiency of the method is concerned, note that the computational times required by the proposed approach vis-à-vis the one related to the standard implementation of the PI technique are reported in Tab. 1. Again, as it can be seen, the use of the asymptotic expansion in the PI approach has drastically decreased the computational cost.

Finally, analyses have been carried out also considering a nonstationary excitation with modulating function in Eq. (35). Pertinent results are shown in Figs. 13 and 14, and comparisons with MCS demonstrate a satisfactory level of accuracy exhibited by the proposed approach.

5.4 System with variable stiffness

As a last application, consider a variable stiffness oscillator, in which the nonlinear function $f(X, \dot{X}, t)$ takes the form

$$f(X,\dot{X},t) = k_0 X\left[1 + r\ sign(X\dot{X})\right]. \tag{43}$$

where k_0 and r are defined parameters of the systems.

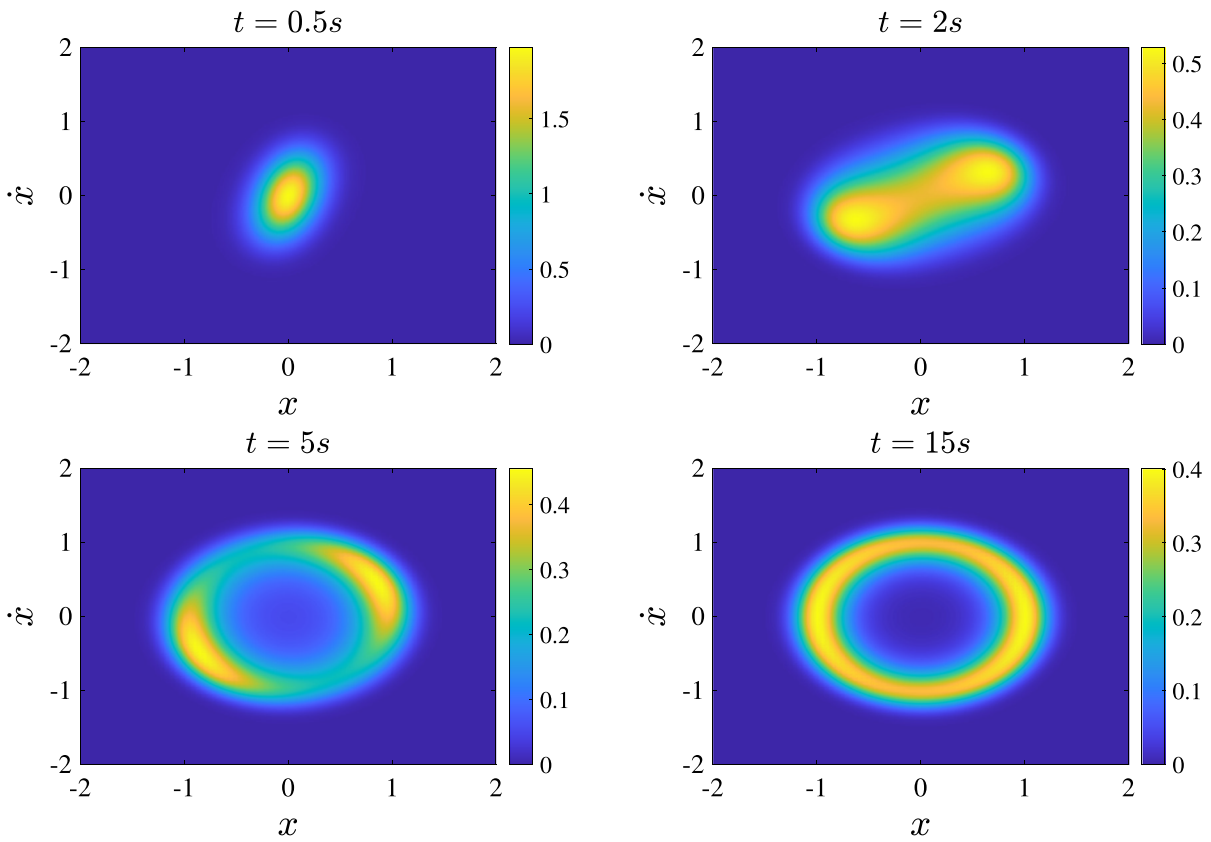

Fig. 6 Response joint PDF of the self-excited oscillator for white noise excitation. Contour plot obtained by the proposed PI approach for different time instants

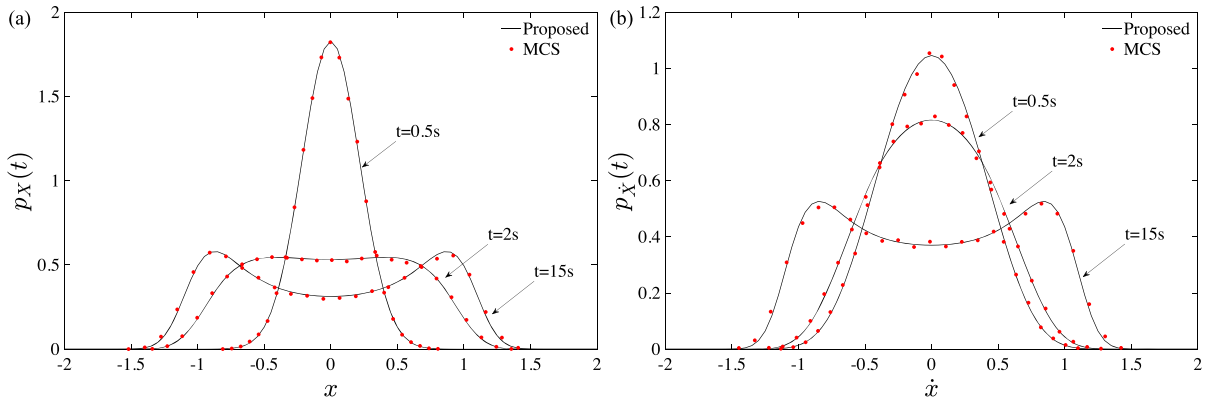

Fig. 7 Response marginal PDF of the self-excited oscillator for white noise excitation. Proposed PI approach (black lines) vis-à-vis MCS data (red dots): **a** Marginal response displacement PDF; **b** Marginal response velocity PDF

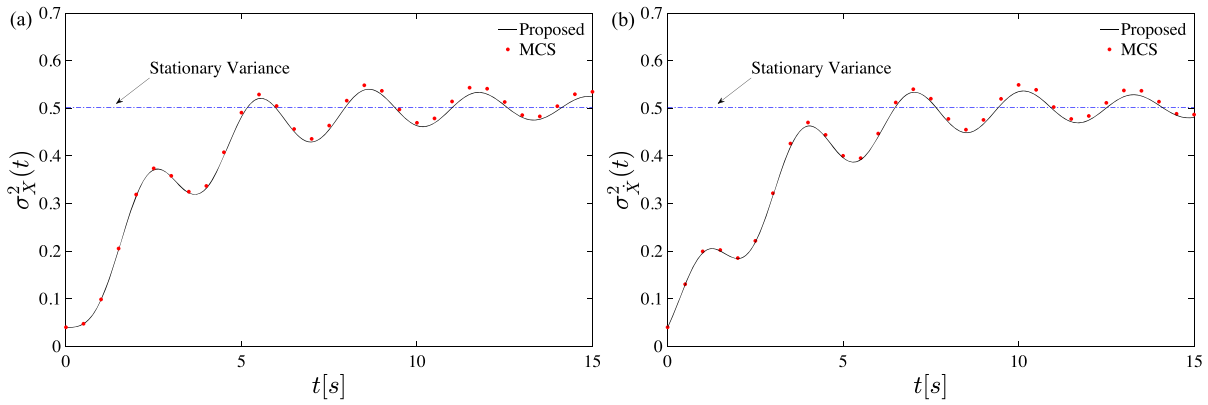

Fig. 8 Nonstationary response variances of the self-excited oscillator for white noise excitation. Proposed PI approach (black line) vis-à-vis MCS data (red dots): **a** Response displacement variance; **b** Response velocity variance

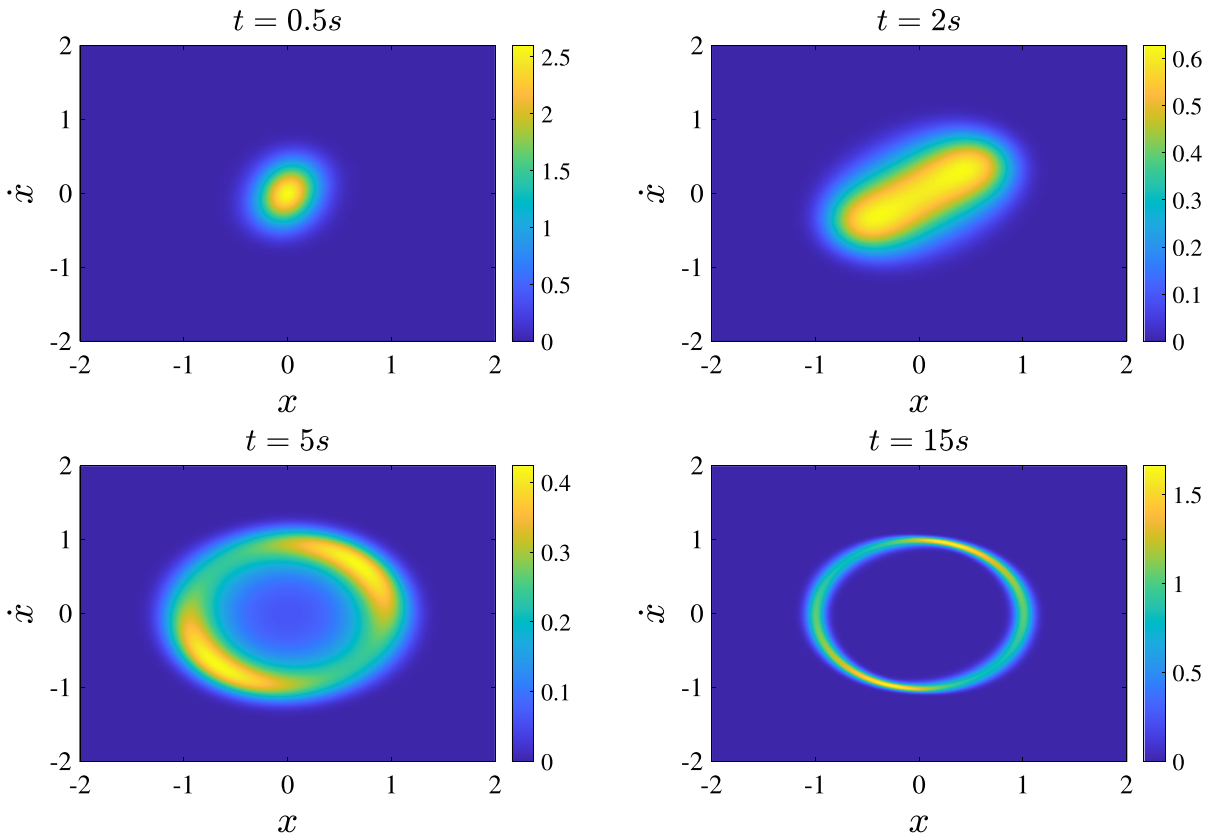

Fig. 9 Response joint PDF of the self-excited oscillator for modulated white noise excitation. Contour plot obtained by the proposed PI approach for different time instants

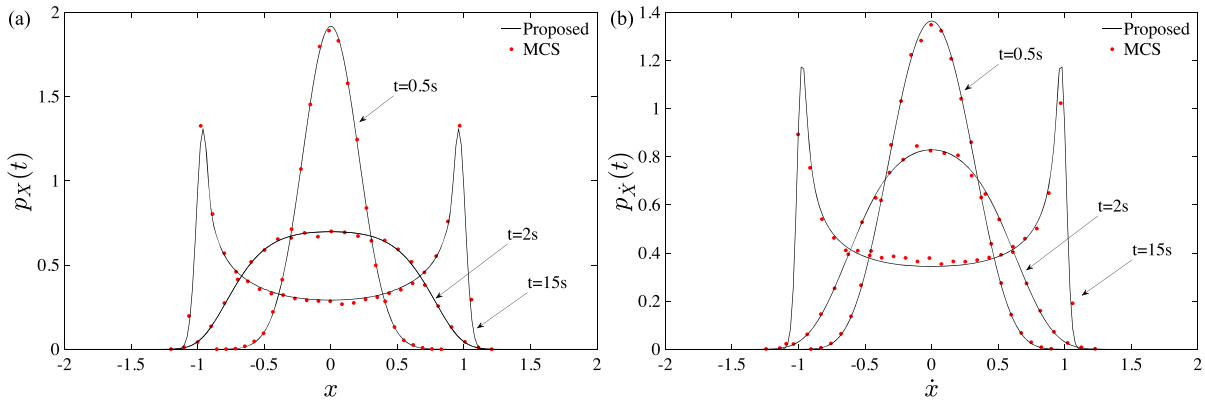

Fig. 10 Response marginal PDF of the self-excited oscillator for modulated white noise excitation. Proposed PI approach (black lines) vis-à-vis MCS data (red dots): **a** Marginal response displacement PDF; **b** Marginal response velocity PDF

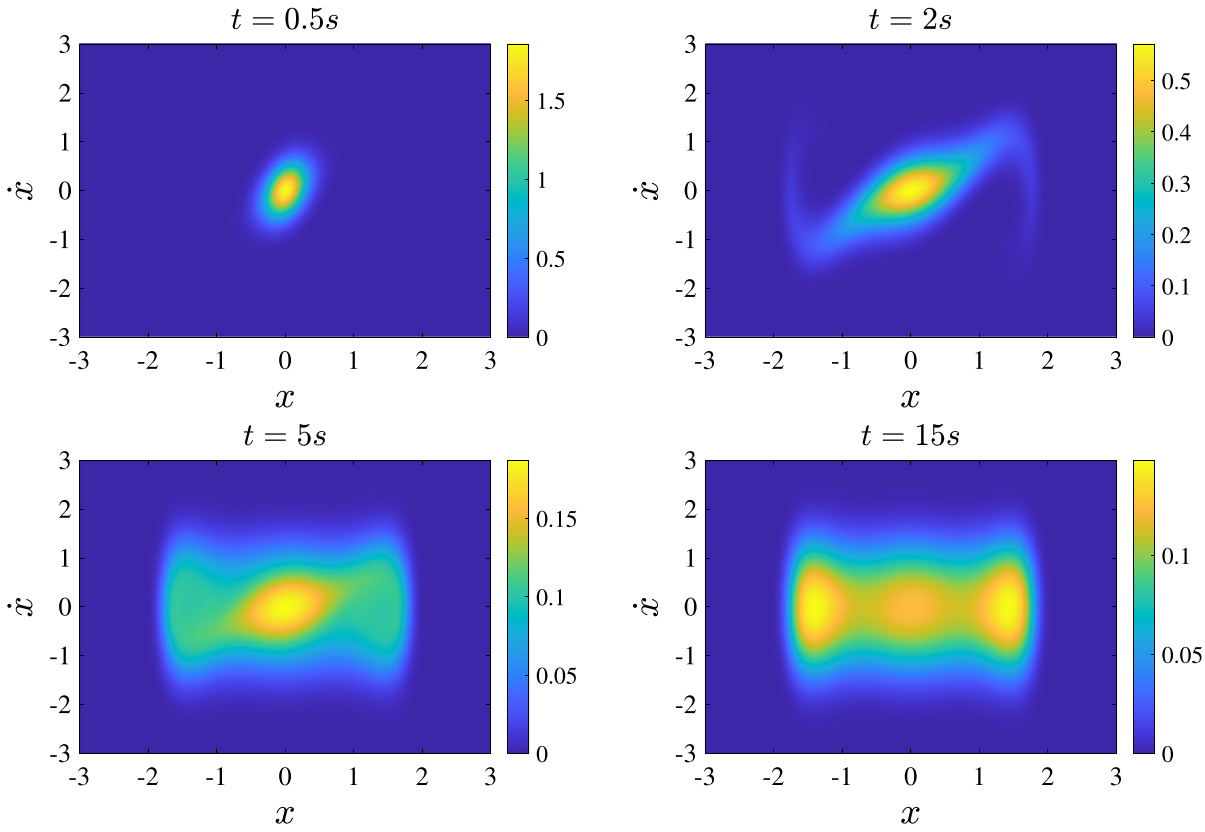

Fig. 11 Response joint PDF of the ship rolling motion for white noise excitation. Contour plot obtained by the proposed PI approach for different time instants

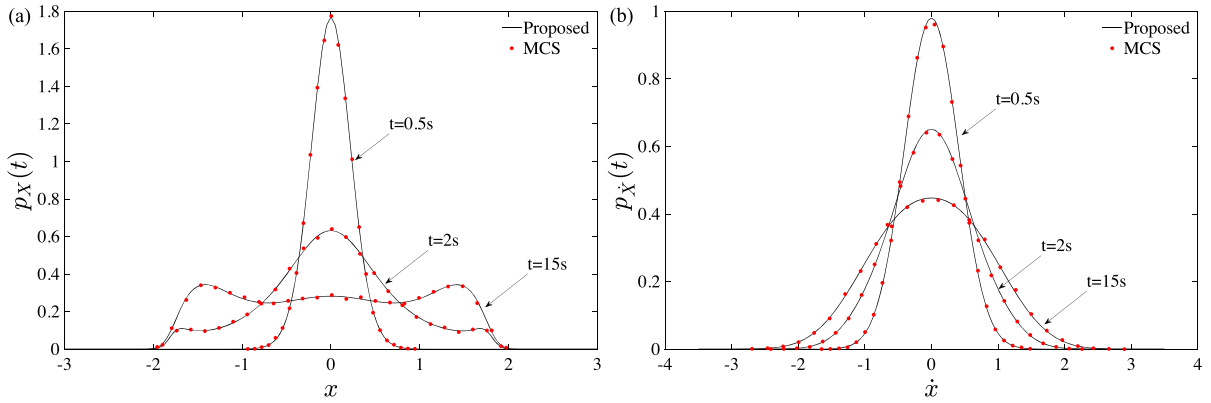

Fig. 12 Response marginal PDF of the ship rolling motion for white noise excitation. Proposed PI approach (black lines) vis-à-vis MCS data (red dots): **a** Marginal response PDF of $X(t)$; **b** Marginal response PDF of $\dot{X}(t)$

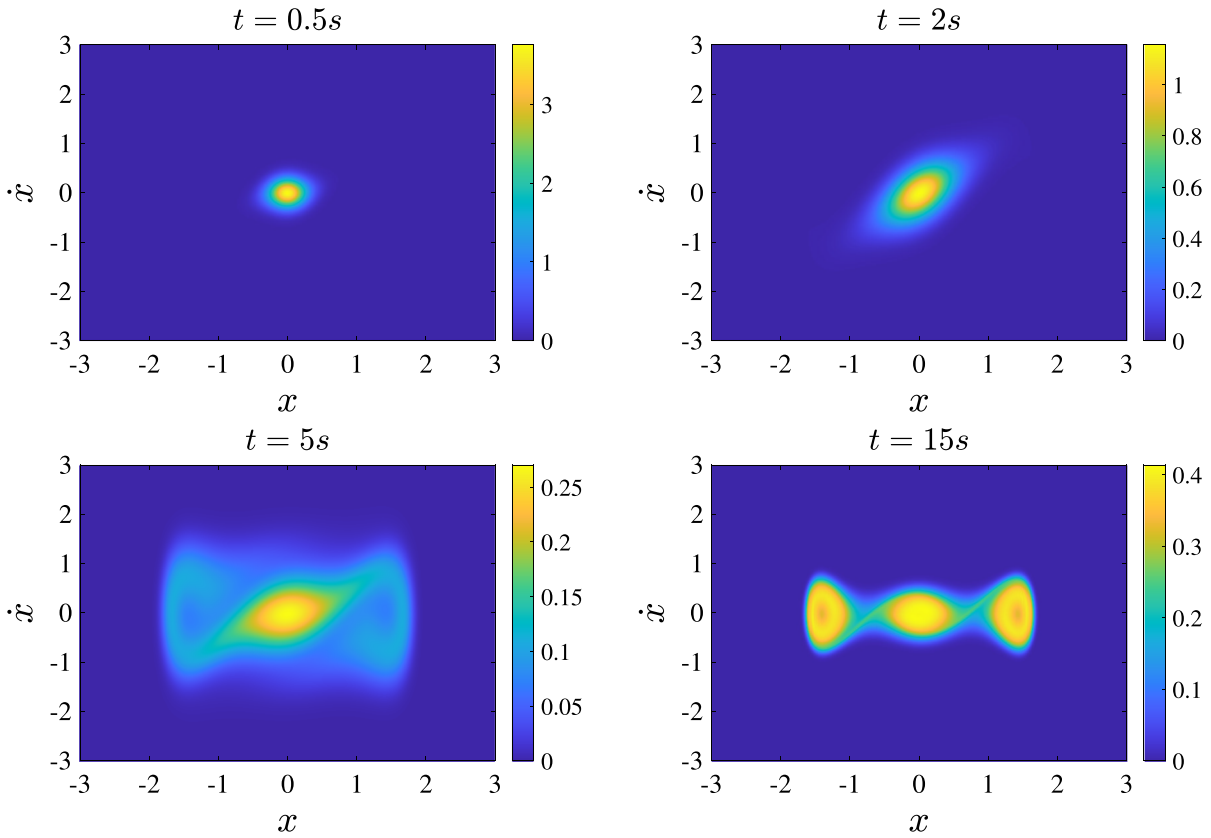

Fig. 13 Response joint PDF of the ship rolling motion for modulated white noise excitation. Contour plot obtained by the proposed PI approach for different time instants

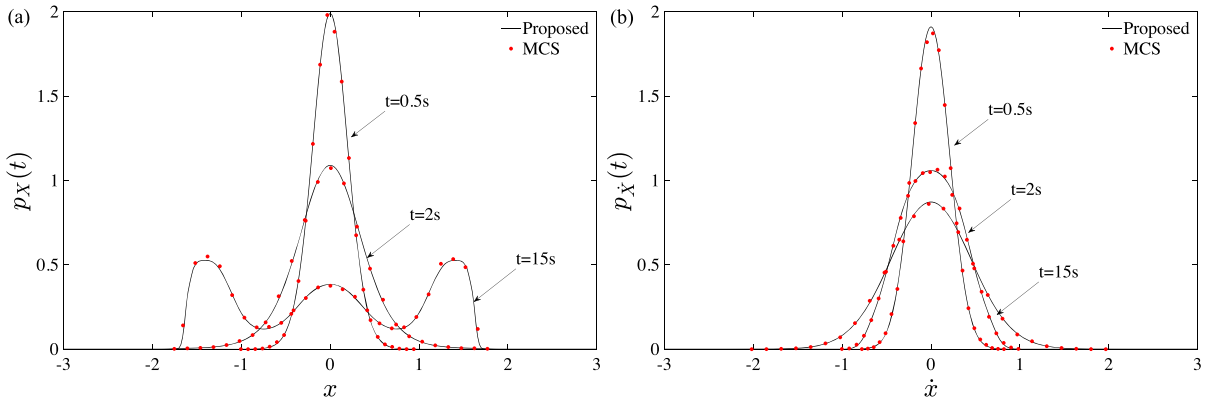

Fig. 14 Response marginal PDF of the ship rolling motion for modulated white noise excitation. Proposed PI approach (black lines) vis-à-vis MCS data (red dots): **a** Marginal response PDF of $X(t)$; **b** Marginal response PDF of $\dot{X}(t)$

It is pointed out that the aforementioned system may be of interest in developing smart materials and it includes a so-called "strong nonlinearity" due to the presence of the discontinuity of the signum function in the nonlinear term, which may be rather challenging to address by using the standard PI approach [24]. In this regard, the proposed procedure has been implemented employing linear interpolation for the evaluation of the terms in Eq. (21) avoiding the use of cubic and spline interpolations as suggested in [24]. Further, with respect to the previous examples, a finer uniform grid and smaller time steps have been chosen, considering $\Delta x = \Delta\dot{x} = 2 \cdot 10^{-2}$ and $\Delta t = 2 \cdot 10^{-3}$ s.

Analyses have been carried out considering the parameters in [24]; that is, $(k_0 = 1, r = 0.5, S_0 = 0.3/2\pi)$.

In this regard, Fig. 15 shows contour plots of the proposed PI-based response joint PDF for different time instants, while in Fig. 16 corresponding marginal response PDF are plotted. The juxtaposition with MCS data reveals a satisfactory level of accuracy in each time instant for both the response marginal PDFs $p_X(t)$ and $p_{\dot{X}}(t)$.

Further, the computational times required by the proposed approach vis-à-vis the one related to the standard implementation of the PI technique are reported in Table 1. As it can be seen, with respect to the previous cases, the computational time has increased due to the finer grid and smaller time steps. Nevertheless, the use of the asymptotic expansion in the PI approach has significantly decreased the computational cost of the standard implementation of the PI technique.

5.5 First-passage analyses

In this section, the accuracy of the asymptotic expansion-based PI approach for the determination of the first-passage probability $P_E(T)$ is assessed by comparisons with pertinent MCS data.

Analyses have been carried out considering the aforementioned four different nonlinear systems, subject to a stationary white noise excitation. In this regard, in Figs. 17, 18, 19 and 20 the log-linear plots of the response marginal PDFs of these systems, evaluated at $(T = 5\,\text{s})$, are shown vis-à-vis pertinent MCS data. Note that, as generally done in the literature, semi-logarithmic plots are employed to more clearly show the accuracy of the proposed approach for small values of the PDFs. As it can be seen, the proposed PI approach-based results satisfactorily agree with corresponding MCS data even at very low magnitude (about 10^{-4}).

Further, Figs. 21, 22, 23 and 24 show the corresponding first-passage probability $P_E(T)$ related to the Duffing nonlinear system (Eq. 36), the self-excited nonlinear system (Eq. 39), the ship rolling motion case (Eq. 42), and the variable stiffness oscillator (Eq. 43), respectively. In this regard, proposed PI-based results have been obtained by using Eq. (36), taking into account Eqs. (33) and (34), employing a time-step $(\Delta t = 10^{-3}\,\text{s})$, whereas MC simulations have been carried out considering 10^6 samples for each case.

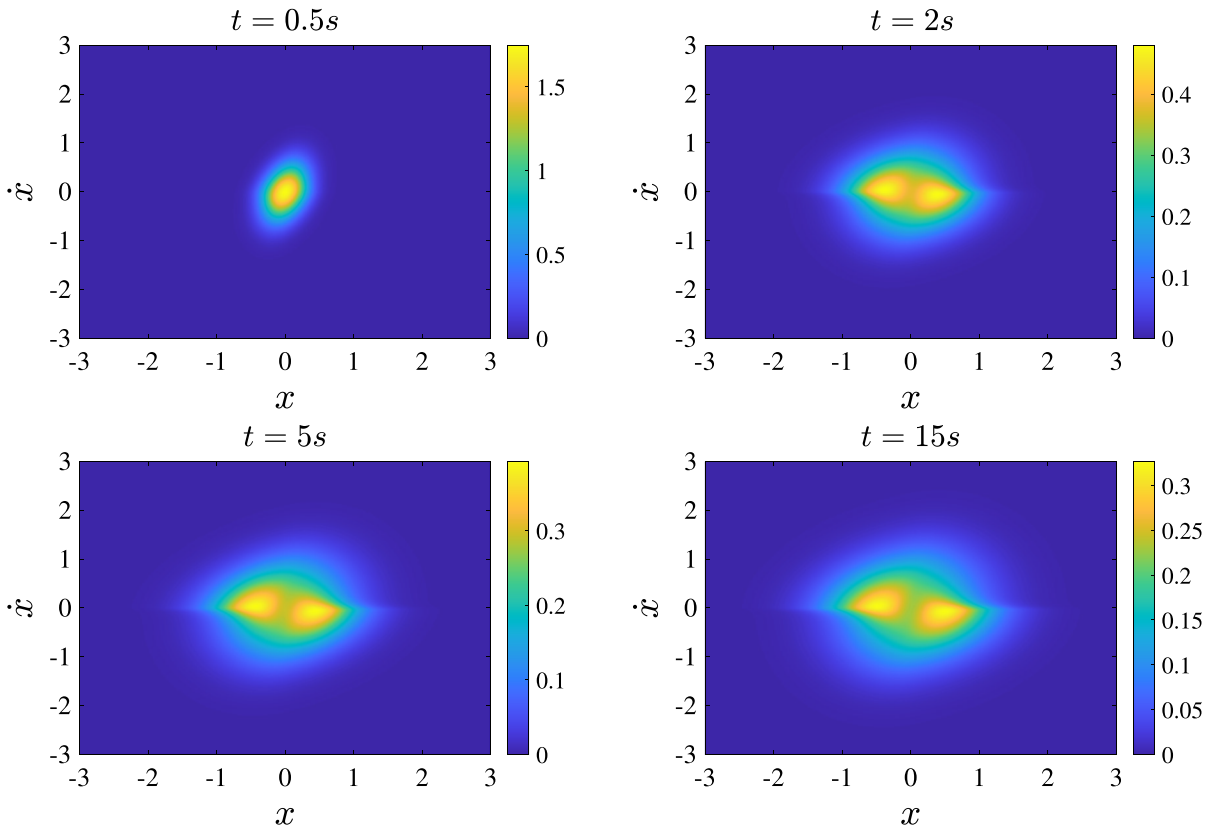

Fig. 15 Response joint PDF of the system with variable stiffness for white noise excitation. Contour plot obtained by the proposed PI approach for different time instants

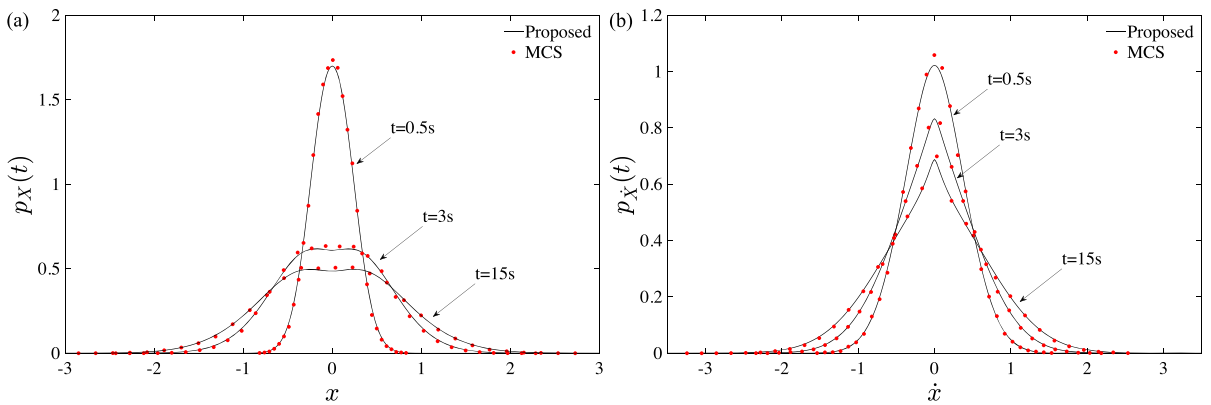

Fig. 16 Response marginal PDF of the system with variable stiffness for white noise excitation. Proposed PI approach (black lines) vis-à-vis MCS data (red dots): **a** Marginal response PDF of $X(t)$; **b** Marginal response PDF of $\dot{X}(t)$

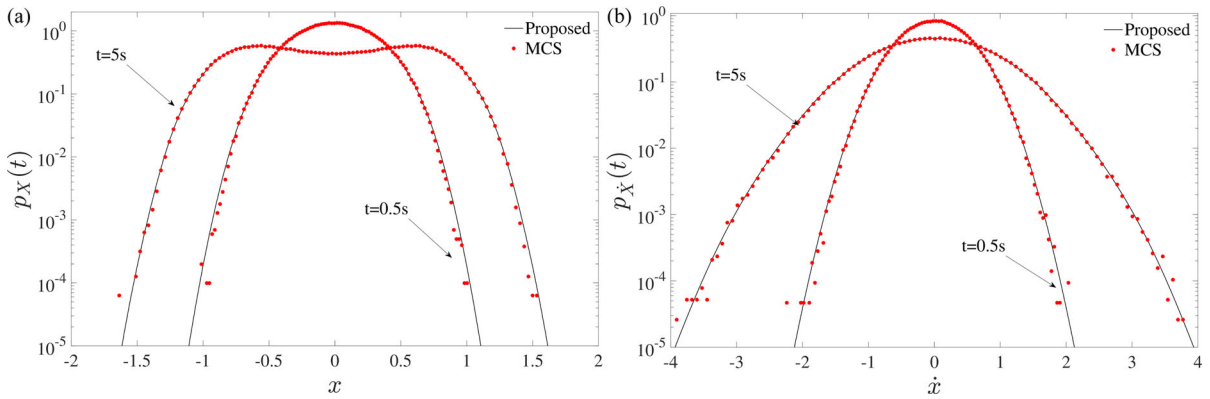

Fig. 17 Response marginal log-linear PDF of the Duffing oscillator for white noise excitation. Proposed PI approach (black lines) vis-à-vis MCS data (red dots): **a** Marginal response PDF of $X(t)$; **b** Marginal response PDF of $\dot{X}(t)$

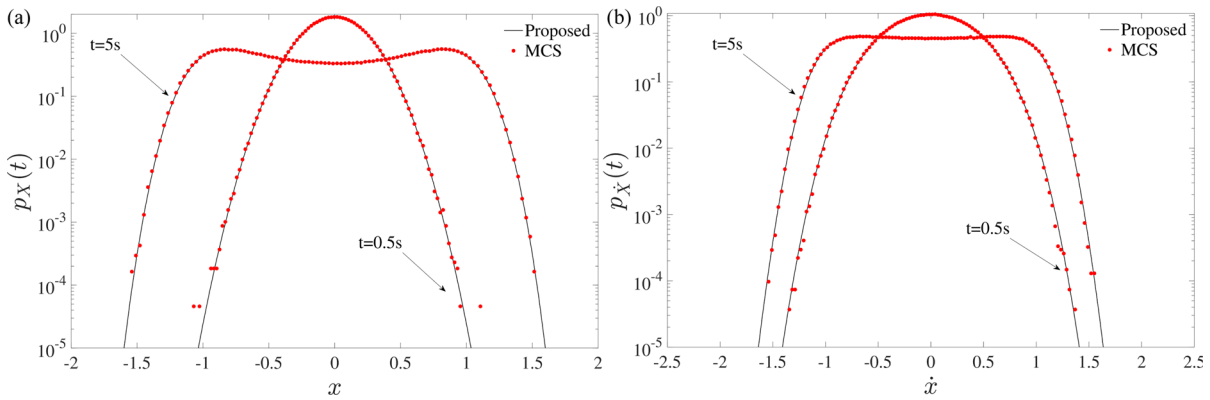

Fig. 18 Response marginal log-linear PDF of the self-excited oscillator for white noise excitation. Proposed PI approach (black lines) vis-à-vis MCS data (red dots): **a** Marginal response PDF of $X(t)$; **b** Marginal response PDF of $\dot{X}(t)$

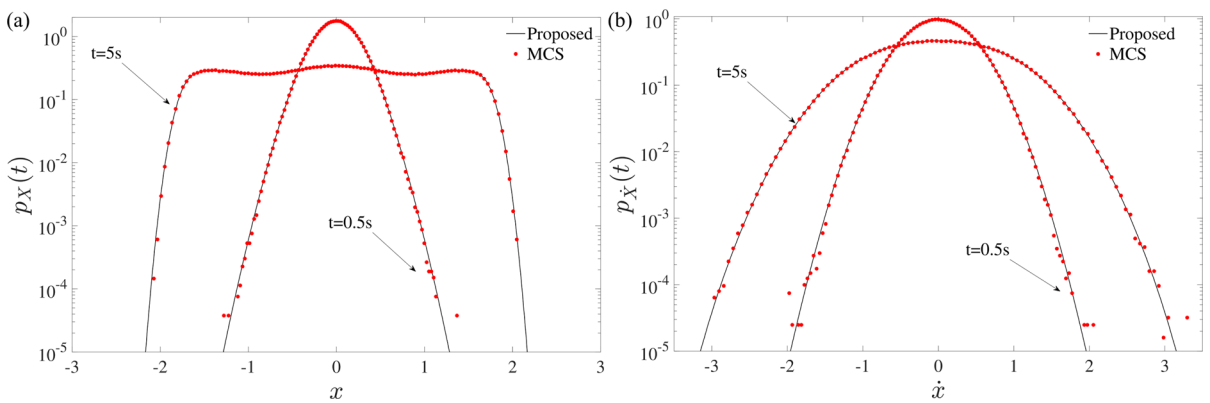

Fig. 19 Response marginal log-linear PDF of the ship rolling motion for white noise excitation. Proposed PI approach (black lines) vis-à-vis MCS data (red dots): **a** Marginal response PDF of $X(t)$; **b** Marginal response PDF of $\dot{X}(t)$

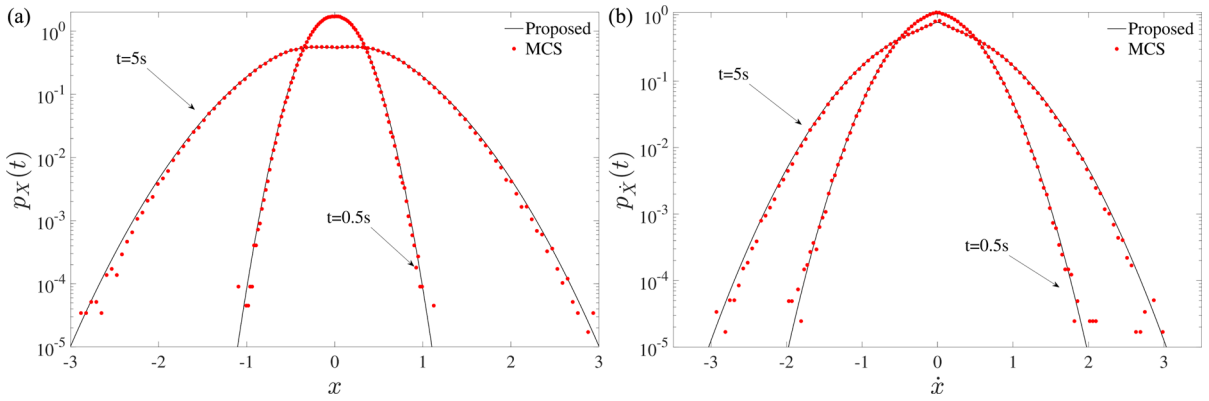

Fig. 20 Response marginal log-linear PDF of the system with varible stiffness for white noise excitation. Proposed PI approach (black lines) vis-à-vis MCS data (red dots): **a** Marginal response PDF of $X(t)$; **b** Marginal response PDF of $\dot{X}(t)$

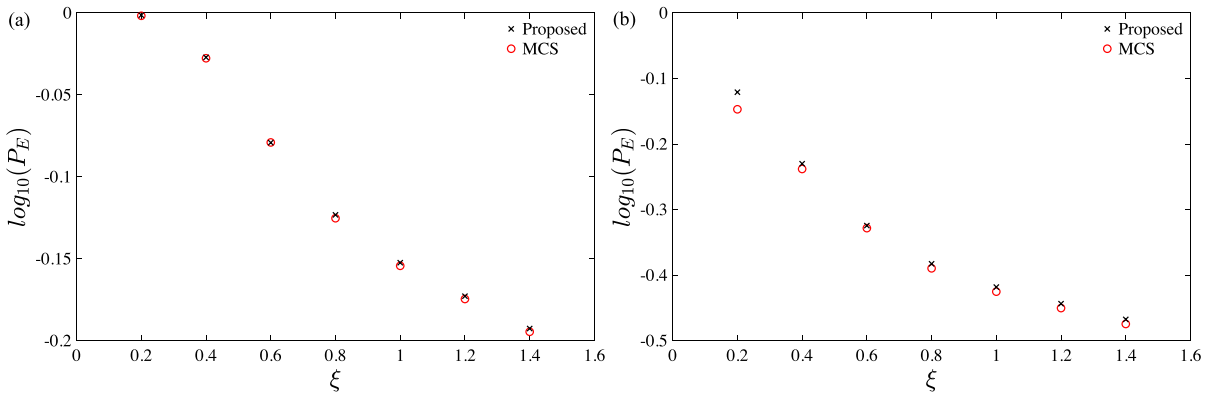

Fig. 21 First-passage probabilities of the system in Eq. (36) for different values of the upper bound ξ. Proposed PI approach (black crosses) vis-à-vis MCS data (red circles): **a** Probabilities for lower bound $\eta = -\xi$; **b** Probabilities for lower bound $\eta = -10$

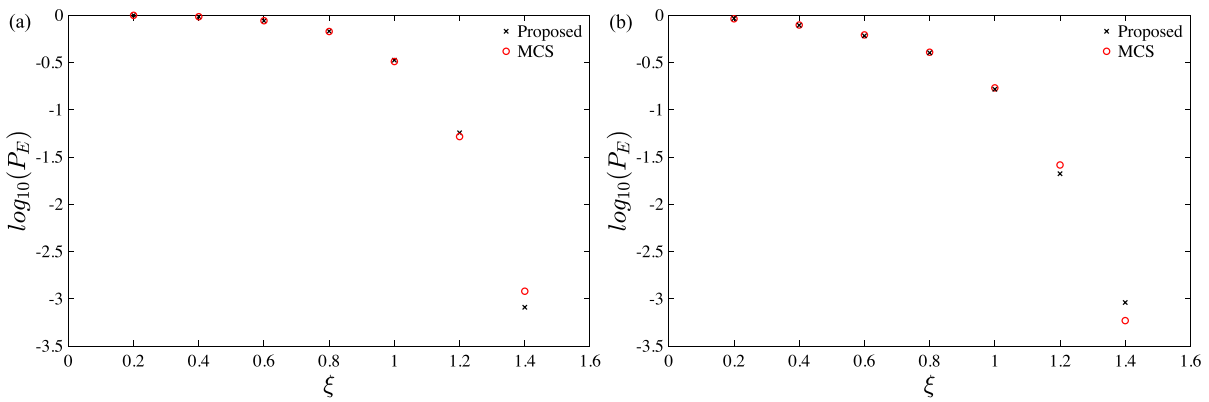

Fig. 22 First-passage probabilities of the system in Eq. (39) for different values of the upper bound ξ. Proposed PI approach (black crosses) vis-à-vis MCS data (red circles): **a** Probabilities for lower bound $\eta = -\xi$; **b** Probabilities for lower bound $\eta = -10$

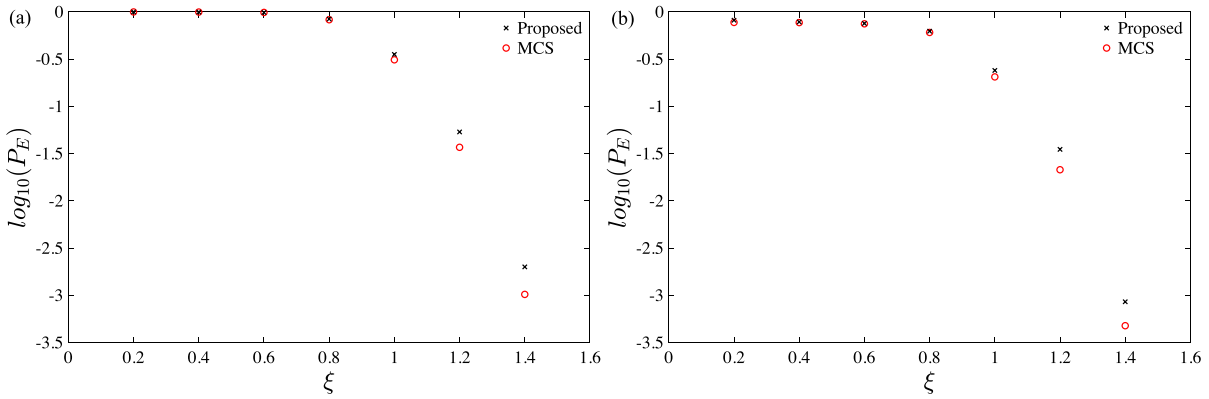

Fig. 23 First-passage probabilities of the system in Eq. (42) for different values of the upper bound ξ. Proposed PI approach (black crosses) vis-à-vis MCS data (red circles): **a** Probabilities for lower bound $\eta = -\xi$; **b** Probabilities for lower bound $\eta = -10$

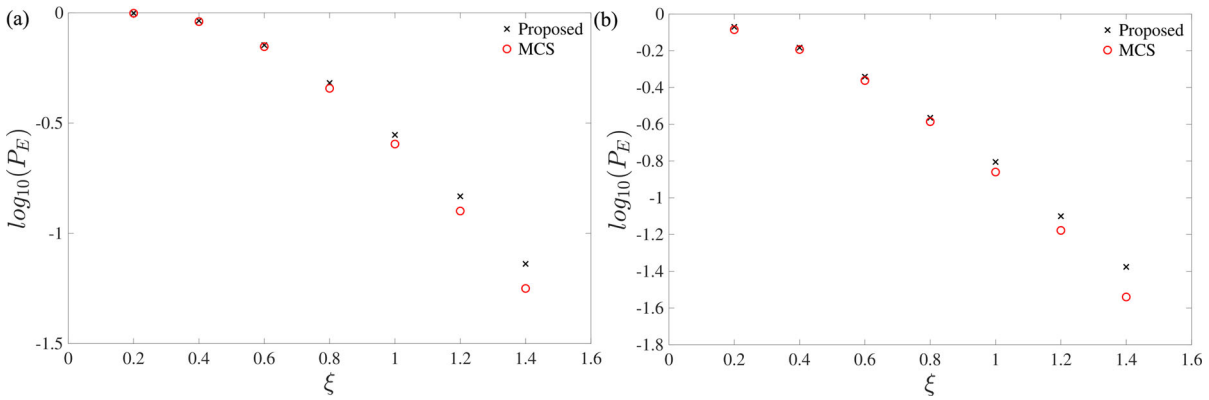

Fig. 24 First-passage probabilities of the system in Eq. (43) for different values of the upper bound ξ. Proposed PI approach (black crosses) vis-à-vis MCS data (red circles): **a** Probabilities for lower bound $\eta = -\xi$; **b** Probabilities for lower bound $\eta = -10$

Note that, for each nonlinear system several values of the upper bound ξ of the interval $[\eta, \xi]$ have been considered. In addition, for each case, two different values of the lower bound η have been employed. Specifically, Figs. 21, 22, 23 and 24a show results of the first-passage probabilities $P_E(T)$ for $(\eta = -\xi)$, while in Figs. 21, 22, 23 and 24b the values of $P_E(T)$ for $(\eta = -10)$ are reported.

As it can be seen in these figures, reasonable agreement is achieved between the proposed PI-based approach and MCS data in all the considered cases for both values of the lower bound η.

In this regard, it can be argued that the high accuracy observed for lower values of ξ is slightly decreased when higher values of the upper bound are considered ($\xi > 1.2$), especially for highly nonlinear systems as in Fig. 23. Undoubtedly, one of the reasons is that, as ξ increases, the first-passage probability decreases rapidly, reaching values of the order of accuracy corresponding to Eq. (32), which is based on a second-order expansion of the integral in Eq. (28).

Notably, the proposed PI approach follows satisfactorily the trend of $P_E(T)$ obtained by MCS, and its level of accuracy is deemed adequate to justify its application for reliability analyses, taking into account that a significant reduction of computational cost is also achieved. In this regard, it is worth mentioning that reliability analyses by MCS generally require a considerable number of samples (of the order of 10^6). Nevertheless, if higher accuracy is necessary, a fourth-order expansion of the kernel in Eq. (29) may be also adopted by employing Eq. (A6).

6 Conclusion

The Path Integral (PI) technique is based on a discretized version of the Chapman-Kolmogorov (CK) equation solved in short time steps for determining the stochastic response of nonlinear systems. This procedure has proven to be reliable and particularly accurate for low-dimensional systems. Nevertheless, its standard implementation can be computationally cumbersome even for single-degree-of-freedom systems and becomes prohibitive as the dimension of the system increases. In this paper, a novel PI approach formulation has been developed based on an analytical asymptotic expansion treatment of the CK equation, generally referred to as Laplace's method of integration. Notably, an approximate closed form solution of the double integrals involved in the CK equation has been derived. In this manner, the repetitive integrations required by the standard implementation of the PI approach have been circumvented and the evolution of the response probability density function (PDF) has been computed by a simple application of the obtained approximate analytical expression in short time steps. Further, appropriate extension for determining the first-passage probabilities of the system has been also presented for the first time. It has been shown that the herein proposed formulation can drastically decrease the associated computational effort by several orders of magnitude, as compared to both the standard PI technique and Monte Carlo solution (MCS). To elucidate the applicability of the technique, several numerical examples have been presented, considering both stationary and modulated white noise excitations with time envelope function. In this regard, nonstationary response PDFs and first-passage probabilities for Duffing and self-excited (Van der Pol-Rayleigh) oscillators, as well as a ship rolling motion nonlinear system, have been included. Further, to show the accuracy of the approach for strongly nonlinear systems, analyses have been carried out also considering a system with variable stiffness comprising a signum type nonlinear term [28]. Comparisons with pertinent MCS data have demonstrated the accuracy and reliability of the procedure. Finally, it is noted that the proposed approach has been developed for two-dimensional nonlinear systems. Nevertheless, in future work it is hoped that the proposed approach could be used to treat relatively high-dimensional multi-degree-of-freedom systems considering, for instance, the case of stochastic excitation only entering in one component of the pertinent stochastic differential equation [46,51].

Acknowledgements A. Di Matteo gratefully acknowledge the financial support received from the PRIN 2022 funding scheme (project 2022TMSPLS - TUNed Dampers Exploitation to Raise VIBration Energy harvesting "TUNDERVIBE") founded by the Italian Ministry of University and Research and European Union-Next Generation EU.

Funding Open access funding provided by Universitá degli Studi di Palermo within the CRUI-CARE Agreement. The authors have not disclosed any funding.

Data availability The datasets generated during and/or analyzed during the current study are available from the corresponding author upon reasonable request.

Declarations

Conflict of interest The authors declare that they have no Conflict of interest.

Appendix A The Laplace's method of integration

Consider an integral of the form

$$\mathcal{I} = \int_a^b e^{-\lambda g(y)} h(y)\, dy, \tag{A1}$$

where the parameter λ is large, and $g(y)$ and $h(y)$ are smooth real-valued functions. Further, assume that the function $g(y)$ has a local minimum at y^* inside the interval $[a, b]$.

On this base, it can be argued that the main contribution to the integral I in Eq. (A1) is mostly originating from the neighborhood around y^*. In this regard, consider the Taylor series expansion of $g(y)$ and $h(y)$

around y^* up to the second order, which yields

$$g(y) \approx g(y^*) + g^I(y^*)(y-y^*) + g^{II}(y^*)\frac{(y-y^*)^2}{2}, \tag{A2}$$

and

$$h(y) \approx h(y^*) + h^I(y^*)(y-y^*) + h^{II}(y^*)\frac{(y-y^*)^2}{2}, \tag{A3}$$

where the apexes (I) and (II) stand for the order of the derivatives with respect to the variable y in Eq. (A1).

Since y^* is a local minimum of $g(y)$, then $g^I(y^*) = 0$. Further, substituting Eqs. (A2) and (A3) in Eq. (A1), yields [54]

$$\begin{aligned}\mathcal{I} \approx\ & e^{-\lambda g(y^*)} h(y^*) \\ & \int_{-\infty}^{\infty} \exp -\lambda g^{II}(y^*)\frac{(y-y^*)^2}{2}\, dy \\ & + e^{-\lambda g(y^*)} h^I(y^*) \int_{-\infty}^{\infty} (y-y^*) \\ & \exp -\lambda g^{II}(y^*)\frac{(y-y^*)^2}{2}\, dy \\ & + e^{-\lambda g(y^*)} h^{II}(y^*) \int_{-\infty}^{\infty} \frac{(y-y^*)^2}{2} \\ & \exp -\lambda g^{II}(y^*)\frac{(y-y^*)^2}{2}\, dy,\end{aligned} \tag{A4}$$

Note that Eq. (A4) now involves only Gaussian integrals which can be solved in closed-form. In this manner, the approximate solution of the integral in Eq. (A1) can be given as

$$\mathcal{I} \approx e^{-\lambda g(y^*)} \sqrt{\frac{2\pi}{\lambda g^{II}(y^*)}} \left[h(y^*) + \frac{h^{II}}{2\lambda g^{II}(y^*)} \right] \tag{A5}$$

Clearly, the accuracy of the approximation can be further improved by retaining additional terms in the expansions in Eqs. (A2) and (A3). In this regard, if a fourth order expansion og $g(y)$ is considered, then Eq. (A5) becomes

$$\begin{aligned}\mathcal{I} \approx\ & e^{-\lambda g(y^*)} \sqrt{\frac{2\pi}{\lambda g^{II}(y^*)}} \Bigg\{ h(y^*) \\ & + \frac{1}{\lambda}\Bigg[\frac{h^{II}(y^*)}{2g^{II}(y^*)} - \frac{h(y^*)}{8}\frac{g^{IV}(y^*)}{g^{II}(y^*)^2} \\ & - \frac{h^I(y^*)}{2}\frac{g^{III}(y^*)}{g^{II}(y^*)^2} \\ & + \frac{5h(y^*)}{24}\frac{g^{III}(y^*)^2}{g^{II}(y^*)^3} \Bigg] \Bigg\}\end{aligned} \tag{A6}$$

References

1. Rubinstein, R.Y., Kroese, D.P.: Simulation and the Monte Carlo Method. Wiley, Hoboken (2007)
2. Proppe, C., Pradlwarter, H.J., Schuëller, G.I.: Equivalent linearization and Monte Carlo simulation in stochastic dynamics. Prob. Eng. Mech. **18**(1), 1–15 (2003)
3. Smyth, A.W., Masri, S.F.: Nonstationary response of nonlinear systems using equivalent linearization with a compact analytical form of the excitation process. Prob. Eng. Mech. **17**(1), 97–108 (2002)
4. Roberts, J.B., Spanos, P.D.: Random Vibration and Statistical Linearization. Dovefr Publications, New York (2003)
5. Roberts, J.B., Spanos, P.D.: Stochastic averaging: an approximate method of solving random vibration problems. Int. J. Non Linear Mech. **21**, 111–134 (1986)
6. Zhu, W.Q.: Recent developments and applications of the stochastic averaging method in random vibration. Appl. Mech. Rev. **49**(10S), 72–80 (1996)
7. Kougioumtzoglou, I.A., Spanos, P.D.: An analytical Wiener path integral technique for non-stationary response determination of nonlinear oscillators. Prob. Eng. Mech. **28**, 125–131 (2012)
8. Kougioumtzoglou, I.A., Di Matteo, A., Spanos, P.D., Pirrotta, A., Di Paola, M.: An efficient wiener path integral technique formulation for stochastic response determination of nonlinear MDOF systems. J. Appl. Mech. **82**, 101005 (2015)
9. Spanos, P.D., Sofi, A., Di Paola, M.: Nonstationary response envelope probability densities of nonlinear oscillators. J. Appl. Mech. **74**(2), 315–324 (2007)
10. Di Paola, M., Falsone, G., Pirrotta, A.: Stochastic response analysis of nonlinear systems under gaussian inputs. Prob. Eng. Mech. **7**, 15–21 (1992)
11. Di Matteo, A., Di Paola, M., Pirrotta, A.: Probabilistic characterization of nonlinear systems under Poisson white noise via complex fractional moments. Nonlinear Dyn. **77**, 729–738 (2014)
12. Chen, L., Liu, J., Sun, J.Q.: Stationary response probability distribution of SDOF nonlinear stochastic systems. J. Appl. Mech. **84**, 051006 (2017)
13. Tian, Y., Wang, Y., Jiang, H., Huang, Z., Elishakoff, I., Cai, G.: Stationary response probability density of nonlinear random vibrating systems: a data-driven method. Nonlinear Dyn. **100**, 2337–2352 (2020)

14. Kovaleva, A.: An exact solution of the first-exit time problem for a class of structural systems. Prob. Eng. Mech. **24**, 463–466 (2009)
15. Di Matteo, A., Spanos, P.D., Pirrotta, A.: Approximate survival probability determination of hysteretic systems with fractional derivative elements. Prob. Eng. Mech. **54**, 138–146 (2018)
16. Zhang, Y., Kougioumtzoglou, I.A.: Nonlinear oscillator stochastic response and survival probability determination via the Wiener path integral. ASCE ASME J. Risk Uncertain. Eng. Syst. B Mech. Eng. **1**, 021005 (2015)
17. Pichler, L., Pradlwarter, H.J.: Evolution of probability densities in the phase space for reliability analysis of non-linear structures. Struct. Saf. **31**, 316–324 (2009)
18. Kougioumtzoglou, I.A., Spanos, P.D.: Response and first-passage statistics of nonlinear oscillators via a numerical path integral approach. J. Eng. Mech. **139**(9), 1207–1217 (2013)
19. Gardiner, C.W.: Handbook of Stochastic Methods for Physics, Chemistry and the Natural Sciences. Springer Series in Synergetics, vol. 13. Springer, Berlin (2004)
20. Risken, H.: The Fokker-Planck Equation, 2nd edn. Springer, Berlin (1996)
21. Wehner, M.F., Wolfer, W.G.: Numerical evaluation of path-integral solutions to Fokker-Planck equations. Phys. Rev. A Gen. Phys. **27**, 2663–2670 (1983)
22. Wehner, M.F., Wolfer, W.G.: Numerical evaluation of path-integral solutions to Fokker-Planck equations. II. Restricted stochastic processes. Phys. Rev. A Gen. Phys. **28**, 3003–3011 (1983)
23. Wehner, M.F., Wolfer, W.G.: Numerical evaluation of path-integral solutions to Fokker-Planck equations. III. Time and functionally dependent coefficients. Phys. Rev. A Gen. Phys. **35**, 1795–1801 (1987)
24. Di Paola, M., Alotta, G.: Path integral methods for the probabilistic analysis of nonlinear systems under a white-noise process. ASCE ASME J. Risk Uncertain. Eng. Syst. B Mech. Eng. **6**, 040801 (2020)
25. Naess, A., Johnsen, J.M.: Response statistics of nonlinear, compliant offshore structures by the path integral solution method. Prob. Eng. Mech. **8**, 91–106 (1993)
26. Lin, H., Yim, S.C.S.: Nonlinear rocking motions. II: overturning under random excitations. J. Eng. Mech. **122**, 728–735 (1996)
27. Barone, G., Navarra, G., Pirrotta, A.: Probabilistic response of linear structures equipped with nonlinear damper devices (PIS method). Prob. Eng. Mech. **23**, 125–133 (2008)
28. Iourtchenko, D.V., Mo, E., Naess, A.: Response probability density functions of strongly non-linear systems by the path integration method. Int. J. Non Linear Mech. **41**, 693–705 (2006)
29. Naess, A., Moe, V.: Efficient path integration methods for nonlinear dynamic systems. Prob. Eng. Mech. **15**, 221–231 (2000)
30. Naess, A., Moe, V.: Stationary and non-stationary random vibration of oscillators with bilinear hysteresis. Int. J. Non Linear Mech. **31**, 553–562 (1996)
31. Cai, G.Q., Lin, Y.K.: Reliability of nonlinear structural frame under seismic excitation. J. Eng. Mech. **124**, 852–856 (1998)
32. Iourtchenko, D., Mo, E., Naess, A.: Reliability of strongly nonlinear single degree of freedom dynamic systems by the path integration method. J. Appl. Mech. **75**, 061016 (2008)
33. Di Paola, M., Santoro, R.: Path integral solution for non-linear system enforced by Poisson white noise. Prob. Eng. Mech. **23**, 164–169 (2008)
34. Pirrotta, A., Santoro, R.: Probabilistic response of nonlinear systems under combined normal and Poisson white noise via path integral method. Prob. Eng. Mech. **26**, 26–32 (2011)
35. Di Matteo, A., Di Paola, M., Pirrotta, A.: Path integral solution for nonlinear systems under parametric Poissonian white noise input. Prob. Eng. Mech. **44**, 89–98 (2016)
36. Bucher, C., Di Matteo, A., Di Paola, M., Pirrotta, A.: First-passage problem for nonlinear systems under lévy white noise through path integral method. Nonlinear Dyn. **85**, 1445–1456 (2016)
37. Bucher, C., Di Paola, M.: Efficient solution of the first passage problem by path integration for normal and Poissonian white noise. Prob. Eng. Mech. **41**, 121–128 (2015)
38. Zan, W., Xu, Y., Metzler, R., Kurths, J.: First-passage problem for stochastic differential equations with combined parametric gaussian and lévy white noises via path integral method. Prob. Eng. Mech. **68**, 110264 (2021)
39. Zan, W., Jia, W., Xu, Y.: Reliability of dynamical systems with combined gaussian and Poisson white noise via path integral method. J. Comp. Phys. **435**, 103252 (2022)
40. Zan, W., Jia, W., Xu, Y.: Response statistics of single-degree-of-freedom systems with lévy noise by improved path integral method. Int. J. Appl. Mech. **14**, 2250029 (2022)
41. Yu, J.S., Cai, G.Q., Lin, Y.K.: A new path integration procedure based on Gauss-Legendre scheme. Int. J. Non Linear Mech. **32**(4), 759–768 (1997)
42. Kumar, P., Narayanan, S.: Modified path integral solution of Fokker-Planck equation: response and bifurcation of nonlinear systems. J. Comput. Nonlinear Dyn. **5**(1), 011004 (2009)
43. Tai, W.-C.: Efficient path integration of nonlinear oscillators subject to combined random and harmonic excitation. J. Comput. Nonlinear Dyn. **17**(6), 061005 (2022)
44. Di Paola, M., Santoro, R.: Path integral solution handled by fast Gauss transform. Prob. Eng. Mech. **24**(3), 300–311 (2009)
45. Sun, J.Q., Hsu, C.S.: The generalized cell mapping method in nonlinear random vibration based upon short-time Gaussian approximation. J. Appl. Mech. **57**(4), 1018–1025 (1990)
46. Alevras, P., Yurchenko, D.: GPU computing for accelerating the numerical path integration approach. Comput. Struct. **171**, 46–53 (2016)
47. Yue, X., Xu, W., Xu, Y., Sun, J.-Q.: Non-stationary response of MDOF dynamical systems under combined Gaussian and Poisson white noises by the generalized cell mapping method. Prob. Eng. Mech. **55**, 102–108 (2019)
48. Peng, J., Wang, L., Wang, B., Dong, S., Xu, W.: Path integration method based on a decoupling probability mapping for fast solving the stochastic response of dynamical systems. Int. J. Non Linear Mech. **156**, 104504 (2023)
49. Peng, J., Wang, L., Wang, B., Jing, K., Xu, W.: A path integration algorithm for stochastic dynamical systems with multiple non-smooth events. Mech. Syst. Signal Process. **185**, 109764 (2023)

50. Sykora, H.T., Kuske, R., Yurchenko, D.: Systematic matrix formulation for efficient computational path integration. Comput. Struct. **273**, 106896 (2022)
51. Gaidai, O., Dou, P., Naess, A., Dimentberg, M., Cheng, Y., Ye, R.: Nonlinear 6D response statistics of a rotating shaft subjected to colored noise by path integration on GPU. Int. J. Non Linear Mech. **111**, 142–148 (2019)
52. Gaidai, O., Dimentberg, M., Naess, A.: Rotating shaft's nonlinear response statistics under biaxial random excitation, by path integration. Int. J. Mech. Sci. **142–143**, 121–126 (2018)
53. Di Paola, M., Alotta, G.: Path integral methods for the probabilistic analysis of nonlinear systems under a white-noise process. ASCE ASME J. Risk Uncertain. Eng. Syst. Part B Mech. Eng. **6**(4), 040801 (2020)
54. Bender, C.M., Orszag, S.A.: Advanced Mathematical Methods for Scientists and Engineers I: Asymptotic Methods and Perturbation Theory. Springer, New York (1999)
55. Miller, P.D.: Applied Asymptotic Analysis. American Mathematical Society, Providence (2006)
56. Di Matteo, A.: Path Integral approach via Laplace's method of integration for nonstationary response of nonlinear systems. Meccanica **54**, 1351–1363 (2019)
57. Di Matteo, A.: Response of nonlinear oscillators with fractional derivative elements under evolutionary stochastic excitations: a path Integral approach based on Laplace's method of integration. Prob. Eng. Mech. **71**, 103402 (2023)
58. Lin, Y.K.: Probabilistic Theory of Structural Dynamics. McGraw-Hill, New York (1967)
59. Caughey, T.K., Payne, H.J.: On the response of a class of self-excited oscillators to stochastic excitation. Int. J. Non Linear Mech. **2**, 125–151 (1967)